2010

Spinal Cord Injury: Exploring the Histology of Electrospun Implants In Vivo

Charles Lin
Virginia Commonwealth University

Spinal Cord Injury: Exploring the Histology of Electrospun Implants In Vivo

A thesis in partial fulfillment of the requirements for the degree of Master of Science in Anatomy and Neurobiology at Virginia Commonwealth University

By

Charles Shin Lin
B.S., University of California, Davis, 2007

Director: Raymond J. Colello, D.Phil
Associate Professor, Department of Anatomy and Neurobiology

Virginia Commonwealth University
Richmond, Virginia
May, 2010

Acknowledgements

I would like to first thank my advisor Dr. Raymond Colello. During my time spent in his laboratory, I have come to a great appreciation for the way he approaches science. He has an amazing ability to construct experiments and has been a wonderful teacher. His enthusiasm and optimism in lab is contagious and I consider myself fortunate to have been able to work so closely with him.

I would also like to thank my committee members. Dr. David Simpson and Dr. Dong Sun, who have been reliable sources of information, support, and have each played an important role in the completion of my research. I know I could always rely on their expertise when needed.

I must thank the members of the laboratory, who were absolutely critical in my success. I could not have done this without all the encouragement, support, and understanding that I have received from my friends and family. Finally, a special thank you goes to Lindsay Kondo, who pushes me every day to be my best.

Table of Contents

Page

List of Figures

Page

Page

List of Tables

Page

List of Abbreviations

3D	Three Dimensional
BSA	Bovine Serum Albumin
BDNF	Brain Derived Neurotrophic Factor
chABC	Chondroitinase ABC
CNS	Central Nervous System
CPSG	Chondroitin sulfate Proteoglycans
DAB	3,3'-Diaminobenzidine
DAPI	4',6-diamidino-2-phenylindole
DRG	Dorsal Root Ganglion
ECM	Extracellular Matrix
EM	Electro Microscopy
FBS	Fetal Bovine Serum
FITC	Fluorescein isothiocyanate
GAG	Glycosaminoglycan
GDNF	Glia Derived Neurotrophic Factor
GFAP	Glial Fibrillary Acidic Protein
HFIP	Hexafluoroisopropanol
HIF	Hypoxia Inducing Factors
LM	Light Microscopy

NGF	Nerve Growth Factor
NT-3	Neurotrophin - 3
PBS	Phosphate Buffered Saline
PDS	Polydioxanone
PGLA	Polyglycolic-Lactic Acid
RBC	Red Blood Cell
SEM	Scanning Electron Micrograph
SCI	Spinal Cord Injury
VEGF	Vascular Endothelial Growth Factor

ABSTRACT

SPINAL CORD INJURY: EXPLORING THE HISTOLOGY OF ELECTROSPUN IMPLANTS IN VIVO

Charles Shin Lin, Master of Science

A thesis in partial fulfillment of the requirements for the degree of Master of Science in Anatomy at Virginia Commonwealth University.

Virginia Commonwealth University, 2010

Raymond J. Colello, D.Phil., Associate Professor, Department of Anatomy and Neurobiology

Spinal cord injury results in loss of motor function and sensory perception. A myriad of obstacles prevent axonal regeneration and ultimately functional recovery in those afflicted with spinal cord injury. Combinatorial strategies addressing many of these obstacles simultaneously have shown promising results. Laboratories investigating contusional spinal cord injuries must overcome the formation of a fluid filled cyst, a physical gap that axons must traverse, at the injury epicenter. To fill the cyst, our lab has generated a 3-D electrospun matrix that is capable of directing neurite outgrowth, delivering neurotrophic support, and reducing the activity of neuroinhibitory compounds. These electrospun matrices were surgically implanted into female Long Evans Hooded rats aged approximately 60 days using a complete transection model of SCI. Following injury, rats with implants showed greater functional recovery than controls. In Chapter 1, we introduce spinal cord injury, the epidemiology, pathology

and potential for regeneration, followed by our novel electrospun implant. Chapter 2 details the materials and methods. In Chapter 3, we relate the functional recovery seen to a histological analysis. The histological analysis consists of three parts: the implant integration into the host, the axons above, in and below the implant, and the functional vascular supply found within the implant. In Chapter 4, we designed a modified implant and discuss the use of this implant *in vivo*. With our modified implant we were able to demonstrate cellular influx and the generation of a vascular network within the implant, but poor axonal regeneration. Finally in chapter 5, I discuss potential future modifications to our electrospun matrix as well as suggestions to consider for improved functional outcome.

Chapter 1

Spinal Cord Injury Anatomy, Pathology, and a combinatorial therapeutic effort

Synopsis:

What is Spinal Cord Injury?

Injury to the spinal cord results in tissue necrosis and axon severing, disrupting communication pathways between the brain and peripheral targets. The result is often a loss of sensation and movement in the affected region. The spinal cord injury (SCI) consists of initial as well as secondary events. Following initial trauma causing tissue loss, secondary injury often further damages the cord and restricts the potential for regeneration. Inflammatory cells infiltrate the injured area and release substrates which drives neurons and glia into apoptosis. The massive cell death from primary and secondary injury results in cell and myelin debris, which inhibit axon growth. Furthermore, glial cells at the border of the injury activate, proliferate and hypertrophy in reaction to the primary insult. The result is a scar-like barrier and the expression of various axon growth inhibitory compounds. The end result of these secondary events is often a fluid filled cyst, which acts as a physical barrier that further complicates the potential for regeneration. These cellular and biochemical events mentioned are only some of many problems in the struggle to understand and treat spinal cord injuries. The

complexity of the injury makes it understandable that no singular approach to spinal cord injury has had success in the past. Combinatorial strategies and therapies that target multiple obstacles offer new hope for the future. This dissertation examines histology behind the implantation of a 3D electrospun matrix that targets multiple therapeutic obstacles in a complete transection model of spinal cord injury in rats. First, we discuss spinal cord anatomy, pathology, epidemiology, and blood supply. Then we introduce many obstacles that prevent regeneration in the damaged spinal cord, and the therapies that have been developed to counter those obstacles.

Introduction

Functional Anatomy of the Spinal Cord

The spinal cord is composed of over a billion neurons and is responsible for the conduction of information between the brain and peripheral targets. This information superhighway comes in the form of an approximately 45cm long soft ovoid shaped tube that runs from the medulla oblongata at the level of the foramen magnum to typically the L1 to L2 vertebral level. White matter is located peripherally within the spinal cord and contains afferent and efferent axon tracts that act as high speed signal conduits. Gray matter located centrally within the spinal cord contain the cell bodies of many of these axons or their interneural connections including those involved with motor control, reflex loops, as well as central pattern generators. In general, afferent sensory axons and tracts are found in the dorsal aspect of the cord while efferent motor axon and tracts are found in the ventral aspect. The spinal cord is protected within the bony

vertebral spinal column. Additionally, the spinal cord is protected and wrapped with the three meninges, the dura mater, the arachnoid mater, and the pia mater. Spinal cord enlargements are found at the cervical or lumbar areas, which are responsible for innervation of the limbs. With the increased circumference of these areas comes lessened space between cord and bony spine. This is the primary reason spinal cord injuries are seen more frequently in the enlargements.

Despite the all encompassing name, spinal cord injuries can be the result of different types actions on the cord. Examples of these are squeezing, tearing, crushing or cutting. A pathological classification was created relating the manner in which the cord was injured to the gross appearance and histology of the cord seen at autopsies. These spinal cord injuries can be clinically classified into four distinct categories. The four groups include solid cord injuries, contusion/cavitation injuries, laceration injuries and massive compression injuries (Bunge et al, 1993).

Solid Cord Injuries

Solid cord injuries represent about 10% of all SCI cases. While no gross defects can be seen, histological analysis typically reveals a loss of normal spinal cord architecture in the injured region (Figure 1.1B). The cause of solid cord injuries is unclear, although inflammation is thought to be a key contributor to their development. It is suggested that light trauma such as stretching or squeezing is enough to trigger inflammation, a component of secondary injury, which can lead to damage in the spinal cord tissue.

Contusion/Cavitation Injuries

The second type of spinal cord injury is contusion/cavitation. This is the most common type of injury and represents approximately half of all cases. These injuries are usually caused by a dislocated vertebra or displaced discs and ligaments pressing into and bruising the spinal cord. Due to the nature of this type of injury, the meninges remain intact despite the fact that there is often visible bleeding within the central gray matter. These areas eventually undergo liquefactive necrosis and as the debris is cleared by inflammatory cells, a fluid filled cyst is formed (Figure 1.1C). At the same time, astrogliosis occurs in which astrocytes proliferate and hypertrophy forming a gliotic scar surrounding the cyst.

Laceration Injuries

Laceration injuries represent about 20% of SCI cases. Laceration of the cord can occur as the result of fragmented vertebra cutting the cord, as well as from stab and gunshot wounds. The key difference between laceration injuries and contusion injuries is the disruption of the meninges (Figure 1.1D). As a result, fibroblasts migrate into the lesion and deposit collagen, creating a mesenchymal scar. It is known that fibroblasts represent yet another barrier to successful axonal regeneration (Webber et al., 2003).

Massive Compression Injuries

Finally, massive compression injuries represent 20% of SCI cases. In a massive compression injury (Figure 1.1E), the cord is completely crushed by a significant force.

As is the case with laceration injuries, the disruption of the meninges represents an additional obstacle for meaningful recovery.

Clinical Classification

Clinical classification of SCI is based on functional outcome. SCI can be classified into complete, incomplete or discomplete. Complete injuries typically result in total paralysis and sensation loss below the level of the lesion. Incomplete injuries result in some functions preserved below the level of injury, which implies that some neuronal tracts have gone undamaged. Finally, discomplete injuries appear complete but patients exhibit some conscious influence on function below the level of injury. This type of SCI is not fully understood.

Blood supply of the spinal cord

The spinal artery enters the intervertebral foramen and divides into three branches outside the spinal canal at each segmental level of the spinal cord: the anterior, posterior and radicular arteries. The radicular arteries enter the dura mater and join with the 3 major spinal arteries: the anterior median longitudinal spinal artery, right posterolateral longitudinal artery, and the left posterolateral longitudinal spinal artery on the surface of the spinal cord. Anastomosis between vessels exist known as the pial plexus, providing local blood flow (Mautes et al., 2000).

Additionally, central arteries originating from the anterior median longitudinal spinal artery travel through the ventral median fissure. The anterior medial longitudinal

spinal artery supplies approximately two thirds of the cross section of the spinal cord. The posterolateral longitudinal spinal artery supplies the remaining one third including the dorsal white matter and dorsal horn. An intermediate zone is supplied by one artery or the other. The spinal cord arteries become arterioles as they enter the cord parenchyma. The arteriole terminates at the level of the capillary. A basal lamina surrounds the endothelial cell. These endothelial cells are often surrounded by the astrocytic foot processes, which help maintain the blood-spinal cord barrier. The blood spinal cord barrier exists at the level of the capillaries, composed of specialized endothelial cells with tight junctions between adjacent endothelial cells (Reese and Karnovsky, 1967).

Treating SCI

Contusion/cavitation type injuries are the most common in clinics. Thus our lab was most interested in this type of injury, the obstacles that are present and the potential therapies to address those obstacles. Following an initial traumatic event to the spinal cord in a percussive injury, a myriad of events occurs.

Inflammation and edema occur quickly. Inflammation within the spinal cord can lead to apoptosis and exacerbate the damage initially sustained (Dusart and Schwab, 1994; Blight, 1992; Blight et al., 1995). Disconnecting the neuron cell body from its neurotrophin source results in additional cell death (Berkelaar et al., 1994) Reactive gliosis occurs in which cell populations surrounding the site of injury undergo hypertrophy and hyperplasia. These cells form a dense cellular network called a gliotic

scar. This gliotic scar represents a mechanical barrier to axon growth (Reier et al, 1983). In addition to mechanically blocking axons, reactive astrocytes release compounds that inhibit neuron growth cones (Apostolova et al., 2006; Pasterkamp et al., 2001; Hagino et al., 2001; Mckeon et al., 1995). This represents a biochemical barrier to axon regeneration. Over time as the cell and axon damage registers, cell death occurs via liquefactive necrosis. The end result of this necrosis is a fluid filled cyst (Figure 1.2). This fluid filled cyst represents a physical gap between the severed axon and its distal target.

Cell death and loss of neurotrophic support

Neurotrophins are small peptides that act on the nervous system through intracellular signaling cascades that promote cell survival, growth, and/or differentiation (Markus et al., 2003). The most widely studied and well understood of the neurotrophins is nerve growth factor (NGF), however a family of growth factors with shared sequence homology also include brain derived neurotrophic factor (BDNF) as well as neurotrophins 3, 4/5 (NT-3, 4/5) (Butte et al., 1998; Ibanez 1994). A multitude of cells have been shown to express these neurotrophins, both in the CNS and peripheral tissues. In the CNS, both neurons and glia can express these growth factors (Pitts and Miller, 2000., Arendt et al., 1995). In the periphery, diverse cell populations can express neurotrophins, of which only a handful are listed: melanocytes, smooth muscle cells, lung fibroblasts, and various endocrine tissues (Levi-Montalcini et al 1995, 1996). These neurotrophins expressed in the target tissue are transported by the

neurons through the axonal projections back to the soma. These neurotrophins act specifically on both high affinity TrkA, B, and C receptors as well as nonspecifically on the low affinity p75 receptors (Bothwell 1995). For example, the TrkA receptor is a transmembrane protein that acts as receptor tyrosine kinase for NGF. Activation of the tyrosine kinase ends in various downstream cascades that effect PI-3, Src, ras, and PLC pathways among others (Saltiel, 1994). The result of TrkA receptor binding leads to archetypal function including cell survival and axon growth cone sprouting. Unlike the Trk receptors, the p75 low affinity receptors are able to bind to all members of the NGF family. While the p75 receptor's exact functions are less clear than the Trk receptor, the p75 receptor binding has been shown to regulate Trk signaling (Dobrowsky et al 1994, 1995). Others state the Trk receptors may act as a sink for excess neurotrophin. Neurons disconnected from their peripheral targets lose these neurotrophic factors that are required for survival and often enter programmed cell death (Berkelaar et al., 1994). It has been shown that neurotrophins in the injured spinal cord react differently temporally. NGF and BDNF levels quickly decline and only transiently increase in the weeks to months following injury. NT-3 levels similarly decline; however regain basal levels by 30 days following injury. In some areas, NT-3 levels have even been shown to be greater than pre-injury (Zhang et al., 2008). Neurotrophins play a critical role in the regenerative process, as it has been shown that exogenous neurotrophins after Central Nervous System (CNS) injury rescue axotomized neurons (Diener and Bregman, 1994; Vejsada et al., 1995).

Reactive astrogliosis and the formation of a gliotic scar

Following a contusional SCI, reactive astrogliosis occurs with cellular hyperplasia and hypertrophy. These cells accumulate close to the site of injury and form a dense cellular formation that is known as a gliotic scar (Fitch and Silver, 2001). This glial scar is characterized not only by dense cellularization, but also by the astrocytic processes that form tight junctions. These tight junctions represent a newly formed glia limitans, which offers structural support in the separation of healthy CNS tissue from the necrotic debris at the injury epicenter. This prevents the spread of necrosis and is beneficial (Fitch et al., 1999; Myer et al., 2006). These astrocytes play an important role in restoring the ionic balance and clearing excess excitatory neurotransmitters that have accumulated in the extracellular environment (Norenberg, 1994). Additionally, the reactive astrocytes are instrumental in remodeling the extracellular matrix (ECM) by laying down deposits of basal membrane. The basal membrane can contract to bring opposing ends of the lesion closer, reducing the size as the debris is cleared. Finally, the gliotic scar provides a cellular scaffold for migrating epithelial and endothelial cells for revascularization of the lesion.

While the gliotic scar has many beneficial functions, it has also been shown to release compounds that inhibit axonal regeneration such as chondroitin sulfate proteoglycans (CSPG). The glial cells within the scar up regulate their expression of CPSG. CPSGs are known inhibitors to axonal regeneration (Mckeon et al., 1995). Chondroitin sulfate proteoglycan is a sulfated glycosaminoglycan (GAG). Proteoglycans are simply polysaccharides attached to a core protein. Depending on the

core protein, the entire molecule takes on a distinctive name. Examples of CPSG molecules include aggrecan, brevican, neurocan, phosphacan, and NG2. CSPG's are found in the ECM of most tissues (Tisay and Key, 1999). These molecules are structural in nature, and important regulators in various biological processes involving cellular recognition, migration and signaling. In the nervous system, CSPGs contribute to the regulation of various developmental processes, stopping neuronal and axonal growth cone migration (Brittis et al., 1992; Cortes et al., 2009). A massive upregulation of these CSPG's occurs following CNS injuries (Lemons et al., 1999). The levels of CPSG stay high with the formation of the gliotic scar (Tang et al., 2003). Although the exact mechanism of inhibition is unknown, it is suggested that the GAG chains are responsible (Morgenstern, 2002). *In vitro* experiments using chondroitinase ABC (chABC), a bacterial enzyme that cleaves these GAG chains, has shown a reduction of the inhibitory activity of CSPGs (Bradbury et al., 2002). In vivo studies using chABC have demonstrated enhanced axonal sprouting, neuroplasticity as well as improved functional recovery in task specific training (Cafferty et al., 2008; Huang et al., 2010; Lee et al., 2010).

Edema and inflammation

Following SCI, the blood brain barrier is often compromised, resulting in a loss of cerebral autoregulation and increase in the permeability of capillaries which leads to accumulation of plasma fluid into the extracellular space. This edema can cause ischemia that may lead to a buildup of metabolites and excitatory neurotransmitters,

causing greater cell death (Stiefel et al, 2005). The disruption of the blood brain barrier evokes a greater post traumatic response by neutrophils and macrophages. In additional, it further complicates the injury cascade as traumatized endothelial and glial cells release vasoactive substances such as nitric oxide and histamines. This facilitates the perfusion of the spinal cord and influences large plasma molecules to enter the cord (Schnell et al., 1999). Inflammatory cells are attracted to the injury site, with the earliest arrival of neutrophils occurring within 12 hours (Dusart and Schwab, 1994). These cells begin to phagocytose much of the cellular and myelin debris. Neutrophils also release cytokines such as IL-8 in the signaling and recruitment of additional inflammatory cells (Chollet-Martin et al., 1996; Beeh et al., 2003). These additional inflammatory cells include resident microglia that hypertrophy and proliferate, as well as infiltrating lymphocytes and peripheral macrophages. Inflammation is a necessary component to wound healing, and while the cleanup of cellular and myelin debris is beneficial, many researchers have claimed that this inflammatory response may be neurotoxic. Within the inflammatory response, neutrophils release many reactive oxidative species and hydrolytic enzymes that cause irreversible damage to the CNS (Hirschberg et al., 1994) and infiltrating lymphocytes are associated with promoting cellular apoptosis (Popovich et al., 1996).

Cyst Formation

Weeks to months following a contusional SCI, a fluid filled cyst forms. Multiple cysts may form as the result of a single initial injury. The cysts are surrounded by a

wall of gliotic scarring and are essentially the final product of the cleanup of debris that occurs. Similar to cysts, syrinxes may also form as a response to injury. Syrinxes differ from cysts in that they have pressure build up, which may cause additional complications. These cavities represent a physical gap in which axons must traverse in order to reconnect with their distal targets.

Vascular issues associated with SCI

Commonly studied in tumors, angiogenesis is one aspect of SCI that is immensely important but often overlooked. The restoration of functional vasculature in the spinal cord following a traumatic event is essential for cellularization and ultimately axonal regrowth to occur. Vascular Endothelial growth factor (VEGF) is just one an example of many factors that are involved with the formation of new blood vessels. Typically in spinal cord injury, local blood flow is disturbed and many cells become hypoxic. The hypoxic environment causes cells to release hypoxia inducing factors (HIF) (Hickey and Simon, 2006). It is believed that mitochondrial generation of superoxide and hydrogen peroxide are required for HIF transcription factors to effectively upregulate gene expression for the release of VEGF (Chandel et al., 1998, 2000). VEGF binds to VEGF receptors on endothelial cells, activating a tyrosine kinase cascade that stimulates preexisting blood vessels to break down their basal laminas using a matrix metalloproteinase. This allows endothelial cells to escape from the parent vessels and form new sprouts into the surrounding extracellular matrix (Rosenburg, 1995). These sprouts extend toward the source of angiogenic stimulus and

anastomoses into loops to become fully functional vessels (Goto et al., 1993; Matsumoto and Claesson-Welsh, 2001).

Following injury to the spinal cord, the blood-spinal cord barrier is often compromised. When this barrier is functional, it prevents immune system cells from entering the central nervous system. This disruption of the blood-spinal cord barrier can expose the spinal cord to neurotoxic elements associated with inflammatory cells (Schlosshauer, 1993). Excitatory neurotransmitters such as glutamate or glycine can also be neurotoxic to cells at high concentrations (Schlosshauer, 1993). The restoration of the blood-spinal cord barrier takes time and it has been shown that small foreign compounds are still present in the CNS up to 28 days post injury (Popovich et al, 1996). As new vessels form, it has been demonstrated that astrocytes are necessary for the restoration of the blood-spinal cord barrier (Whetstone et al., 2003).

All of the events above represent obstacles to successful spinal cord regeneration. Due to the complexity of the injury and pathology in the hours to weeks following, singular approaches have not had success in the past. Combinatorial strategies offer new hope for the future. Our lab has devised a strategy that addresses many of the obstacles to spinal cord injury.

A novel therapeutic strategy

The bridge

Contusion injury to the spinal cord results in liquefactive necrosis of the tissue at the site of injury and often the formation of a fluid filled cyst. This fluid filled cyst is a

physical gap in which axons can not cross. This is often the endpoint of contusional SCI and must be addressed for functional recovery. Research groups have explored the use of varying bridging materials to fill the cyst including: stem cells (McDonald et al, 1999; Akiyama et al., 2002), support cells (Xu et al., 1995; Li et al., 1997), autologous grafts (von Wild and Brunelli, 2003; Houle et al., 2006), embryonic grafts (Reier et al., 1986) or synthetic substances (Tsai et al., 2004; Wen and Tresco, 2006).

While many of these approaches have shown axon growth, few axons have been able to reach the tissue on the opposing end of the bridge. In creating an appropriate bridge for axons in the healing SCI scenario, the material must be biocompatible and allow if not direct axons to grow directionally across. The bridge must be three dimensional and fill the extent of injury, while still porous enough for axons and cells to infiltrate. Finally, this bridge should be compatible with a method for delivery of compounds beneficial to neuroprotection or axonal regeneration.

One method that fulfills all of these requirements is a process called electrospinning. Electrospinning uses a high voltage electric field to generate fine fibers that are deposited on a grounded rotating mandrel to form a cloth like matrix (Bowlin et al., 2002). The electrospinning apparatus is shown in figure 1.3A. These fibers can be composed from extracellular matrix proteins or synthetic polymers. Properties of these electrospun structures, such as fiber diameter, porosity and alignment can be adjusted (Fridrikh et al., 2003). Electrospinning has been used in tissue engineering in many different applications such as dermal implants or synthetic vessels (Stizel et al., 2001; Sun et al., 2005). The synthetic polymer chosen for use in

spinal cord injury is a resorbable suture material polydioxanone (PDS). PDS is biocompatible and has a lifespan *in vivo* of approximately 6 months (Molea et al, 2000; Boland et al., 2005).

A drawback to the use of the electrospinning apparatus is the inability to create an implant that matches the size and morphology of the spinal cord. To address this issue, a modification was made to the ground as shown in figure 1.3B. The mandrel was replaced with two grounded posts, resulting in the fibers whipping around each post in succession and creating a cylindrical scaffold with the fibers aligned along its length. A Scanning Electron Micrograph taken of the fibers is shown in figure 1.4, displaying the porosity of these fibers in the matrix.

These bridges were tested for their ability to support neurite outgrowth *in vitro*. Using dorsal root ganglions (DRG) taken from neonatal rats, we were able to show that not only could DRGs survive on these electrospun matrices, but that the neurites were also directed by the alignment of the fibers (Figure 1.5A)(Chow et al., 2007). However, these outgrowths soon degenerated without appropriate trophic support (Figure 1.5B). In order to support axons growing through the electrospun matrix, the matrix had to be supplemented with neurotrophic factors that promote the survival of neurons. Such neurotrophic factors play a significant role in the CNS following trauma (Dougherty et al., 2000; Krenz and Weaver, 2000). In order to supplement our electrospun implant with bioactive neurotrophic factors, alginate was used as a vehicle for delivery. Alginate is a gum found in cell walls of certain brown algae and seaweeds that is used in industrial, food processing, and biomedical applications such as a waterproofing,

thickening, or detoxification agent. Alginate is biocompatible and can be utilized *in vivo*. Nearly all proteins of interest can be encapsulated in alginate and dehydrated, providing sustained release of protein upon hydration (Noushi et al., 2005). We could show the extent of protein incorporation by simply placing a FITC conjugated protein in the alginate (Figure 1.6). Furthermore, we ran a simple dorsal root ganglion bioassay experiment to demonstrate that these proteins encapsulated within alginate by electrospraying remained bioactive upon rehydration (Ayres et al., 2010). NGF was clearly shown to be released from alginate beads *in vitro* (Figure 1.7), and in a form that could effect the growth of the DRG (Figure 1.8). A final component to our bridge required we address the issue of the inhibitory compounds being released by the reactive astrocytes in the gliotic scar surrounding the cyst. Chondroitinase ABC (chABC) is an enzyme that cleaves the GAG chains from the neuroinhibitory CSPGs. It has been shown that this functions to decrease the inhibitory activity, and several *in vitro* as well as *in vivo* studies have established that this enzyme facilitates axonal regeneration. In a series of experiments, we demonstrated that we could incorporate chABC into our electrospun implants and the enzyme remained bioactive (Figure 1.9).

Having demonstrated the potential various beneficial utilities of using an electrospun matrix in a spinal cord injury setting, we hypothesize that by using a 3-D airgap electrospun matrix in a rat given a complete transection spinal cord injury, we could increase functional recovery and correlate the increase to axon and vascular growth into the implant.

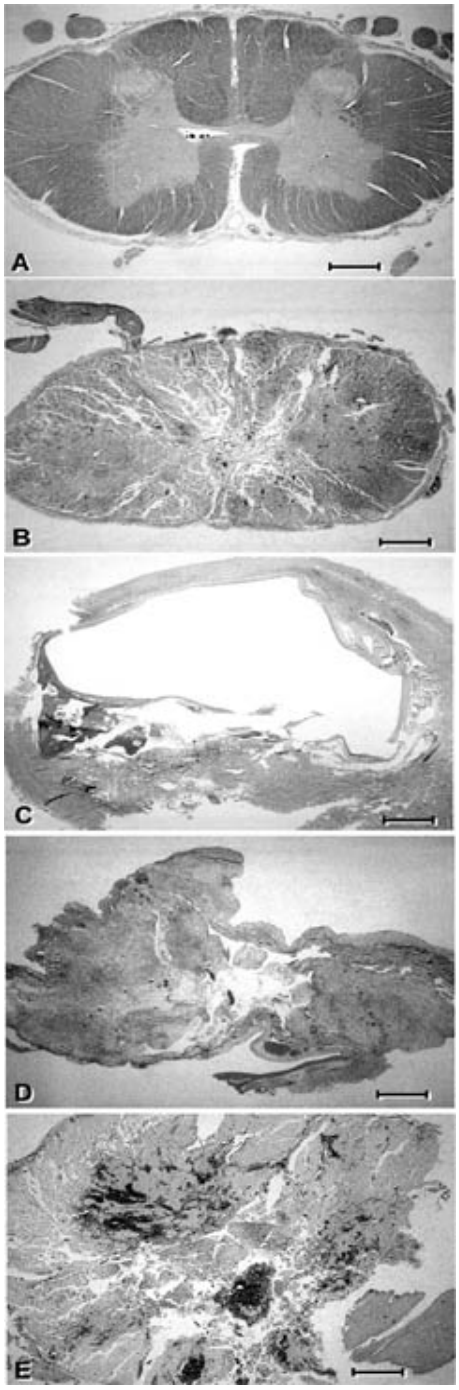

Figure 1.1. Pathology of the Spinal Cord. Histology (A) Cross section of a normal human spinal cord at the cervical level. (B) Loss of spinal cord architecture seen in solid cord injuries. (C) Formation of fluid filled cavities in contusion/cavitation injuries. (D) Disruption of Pia in laceration injuries. (E) Loss of tissue and hemorrhage in massive compression injuries. Scale Bars (A to E) = 2 mm. (Norenberg et al., 2004)

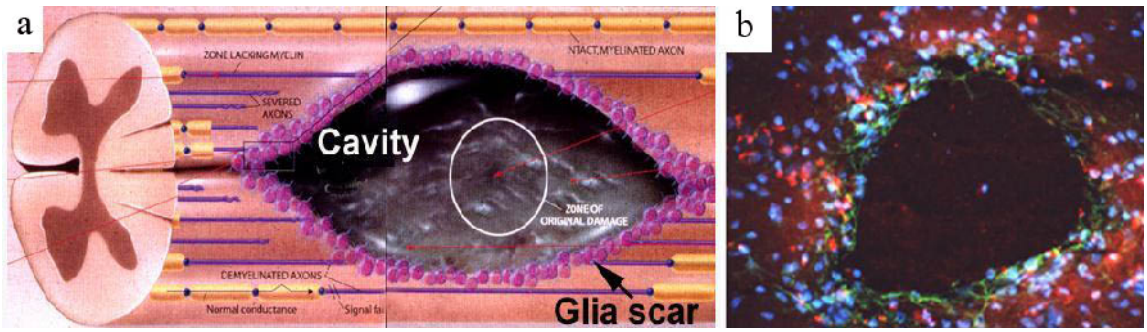

Figure 1.2. The Cystic Cavity. (A) A schematic of the glial scar and cavity that form post injury. (B) Section of an injured rat spinal cord 2 weeks following injury. Astrocytes are shown in green, cell bodies in blue and chondroitin sulfate proteoglycans in red. Figure 1a was modified from McDonald et al., (1999).

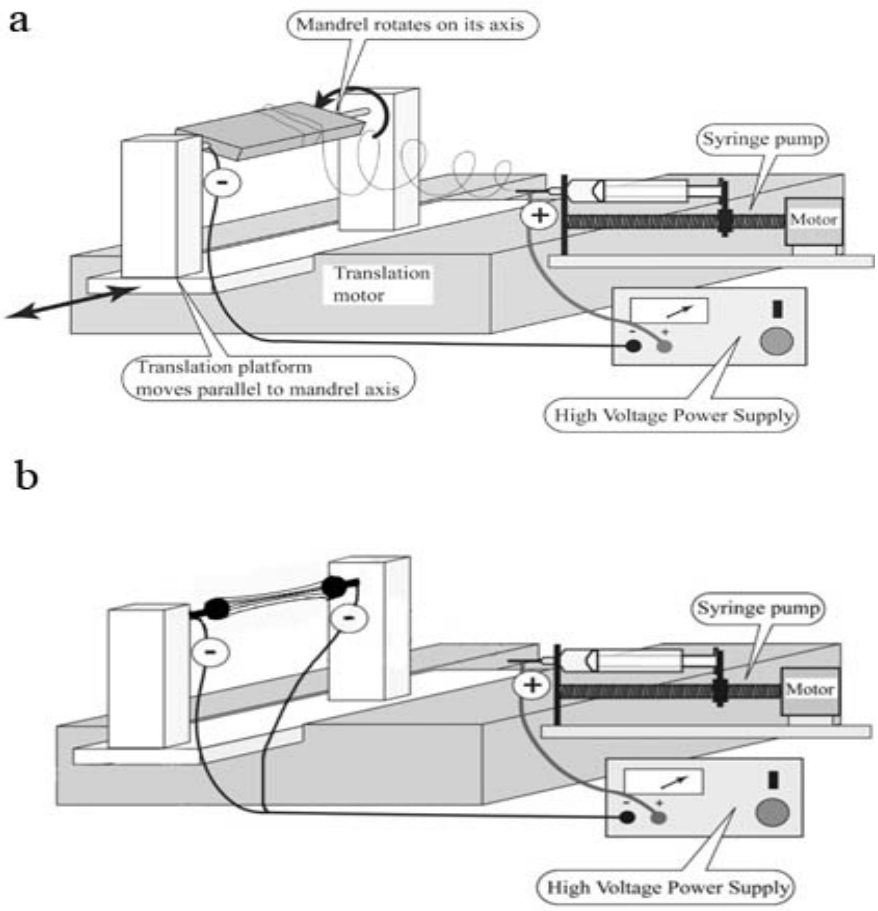

Figure 1.3. The Electrospinning Apparatus. Key system components include a solution reservoir (syringe), nozzle (18-gauge, blunted, metallic needle), high-voltage DC power supply, and grounded target (rotating mandrel). (A) The original electrospinning apparatus with rotating mandrel for fiber collection. (B) The airgap electrospinning apparatus. The grounded mandrel is replaced with two grounded posts.

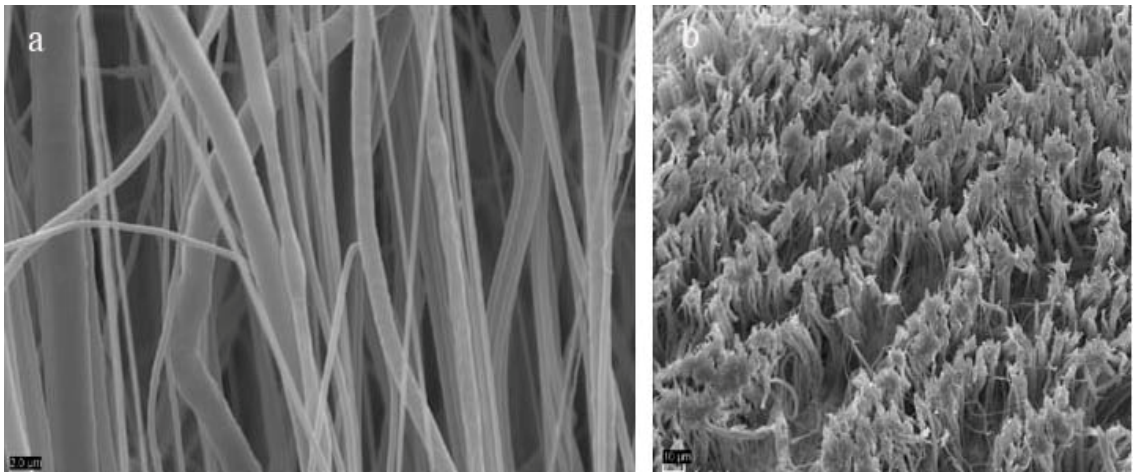

Figure 1.4. SEM of PDS Matrix Monofilaments. (A) SEM showing aligned fibers in a representative matrix. Fiber diameters can be seen here varying greatly, but generally held to under 3 μm. (B) SEM taken of a PDS matrix cut in cross section. Fibers are packed densely but with porosity for cells and axons to grow through. Scale bar (A)=2 um, (B)= 10 um.

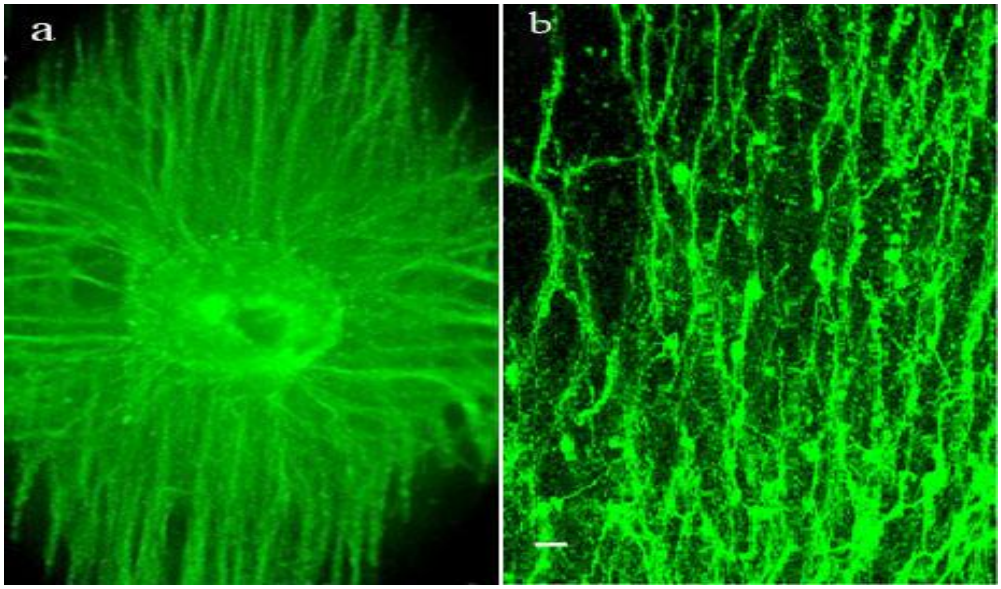

Figure 1.5. Electrospun matrices support neurite outgrowth. (A) A pinned DRG immunostained for TuJ1 on an electrospun matrix. Directionality of neurite outgrowth is influenced by aligned fibers. (B) A pinned DRG's neurite outgrowths are seen degenerating 1 week without neurotrophic support. Scale bar B = 10μm

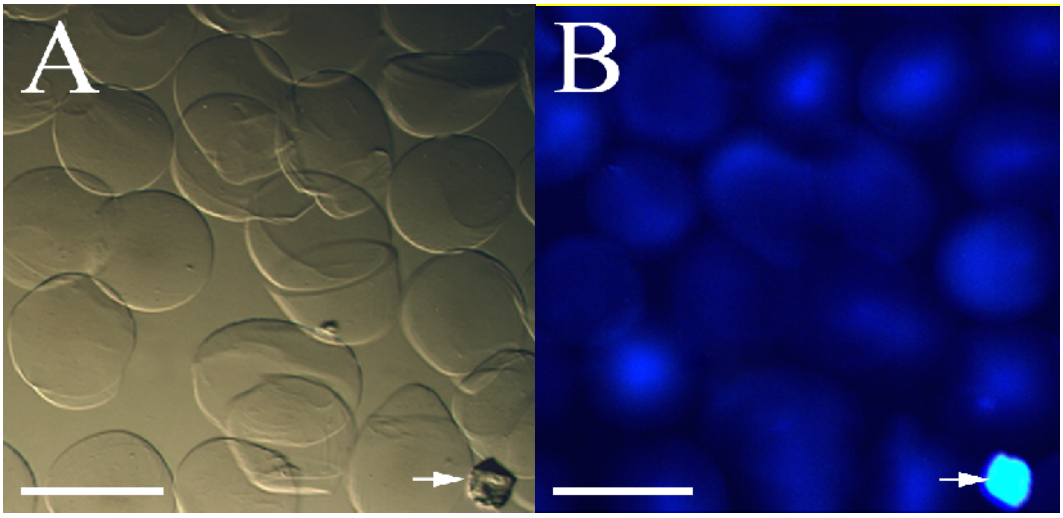

Figure 1.6. Alginate microspheres. (A) A light microscopic image of the alginate carrier beads. (B) A wide-field fluorescence image of the same alginate carrier beads showing the incorporation of a fluorescent protein. The white arrows point to the same piece of debris, indicating the same field of view in both images. Scale Bars (A and B) = 10 μm.

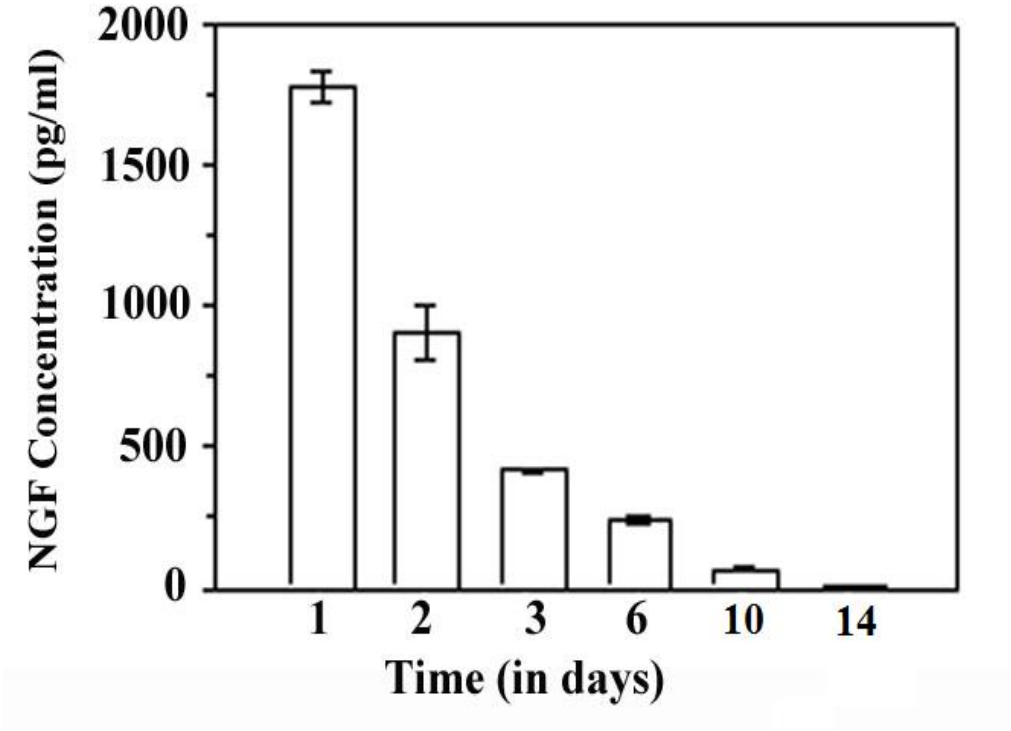

Figure 1.7. Alginate microsphere release kinetics for NGF. NGF ELISA measures NGF released by alginate beads + NGF over 6 time points. NGF release is greatest in the first 3 days following hydration, but continues to release NGF up to 14 days.

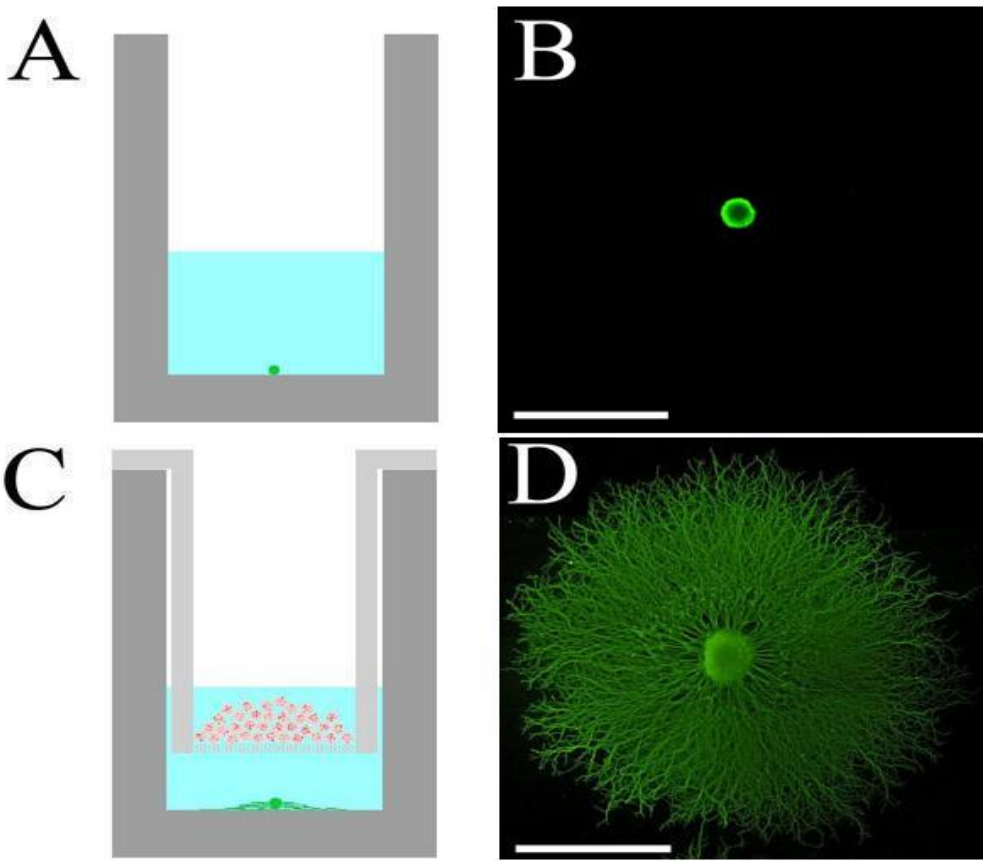

Figure 1.8. Results for NGF bioassay. Results of Bioassay on Alginate encapsulated NGF on DRG outgrowth. (A) and (C) are schematics equating to (B) and (D) respectively. In (B) no outgrowth is seen in media without NGF. In (D), robust outgrowth of neurites is seen when NGF is delivered in the alginate carrier beads. Scale bar = 500 μm

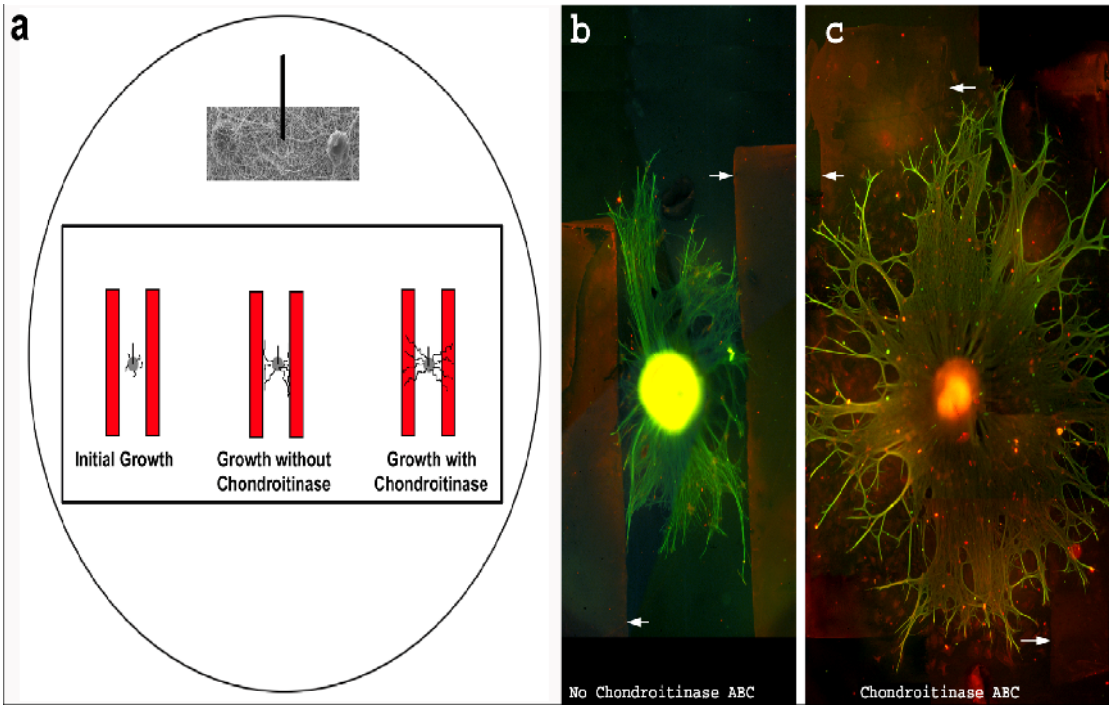

Figure 1.9. Results for chABC strip bioassay. Strip bioassay of dorsal root ganglia (green) grown between aggrecan lanes (red) for 7 days in culture. Aggrecan is a CSPG, is a known axon inhibitor. (A) is a schematic of the strip bioassay. (B) and (C) are the corresponding results. In the absence of chABC, DRG neurites were inhibited from growing on aggrecan lanes. However; the presence of a chABC in the matrix reduces the inhibition. Arrows denote boundaries of aggrecan. Scale Bars (B and C) = 500 μm.

Chapter 2

Materials and Methods

Air Gap Electrospinning:

PDS (monofilament suture, Ethicon) is dissolved in 1,1,1,3,3,3 hexafluoro-2-propanol (Sigma-Aldrich) at a concentration of 100 mg/ml. This electrospinning solution is loaded into a 5-ml syringe (capped with an 18-gauge blunt end needle) that is mounted into a syringe pump. The needle is connected to a high voltage, low amperage DC power supply (Spellman CZE1000R) via an alligator clip and charged to 22kV. A 2 pole system consisting of grounded horizontal piers that are separated from one another by a 5-10 cm gap (Figure 1.2B) is used (Ayres et al., 2008). This system produces cylindrical constructs composed of individual fibers with cross-sectional diameters ranging between 1 to 3 μm. These fibers are deposited across the gap that separates the grounded piers into arrays that are oriented in parallel with the long axis of the constructs.

Creation of PGLA capsule:

Following the creation of an electrospun matrix with the airgap electrospinning technique, a second copolymer Polyglycolic-Lactic Acid (PGLA) consisting of 50% polyglycolic acid and 50% polylactic acid is prepared as stated above. The 2 pole system is removed and a grounded plate is placed at a distance such that the newly formed matrix is between the charged needle and grounded plate. When the voltage is

applied, the PGLA copolymer is electrosprayed towards the grounded plate. The PDS matrix is rotated so that PGLA is able to coat evenly.

Creation of Alginate Beads containing growth factors:

Alginate beads were generated with an electrospraying technique (Ayres et al., 2010). An appropriate quantity of the solute of interest was added to 300 µl solution of 0.005-mg/ml sodium alginate and 0.005-mg/ml protease-free bovine serum albumin (used as a carrier). The solution was then loaded into a 1-ml syringe tipped with an 18-gauge blunt-end needle (Kontes) installed onto a syringe driver. The needle was connected to an anode of a high voltage direct current power supply (Spellman CZE1000R) via a wire outfitted with an alligator clip. A 150-mm glass Petri dish filled with 2% calcium chloride solution was placed on a metal plate. By switching the power supply on, an electric field was formed which pulls the alginate solution out of the syringe as an aerosol mist and into the calcium chloride solution. Upon contact with the calcium the alginate forms into a bead that traps the solute (growth factor) of interest. The beads were collected, washed by centrifugation in a 2% calcium chloride solution supplement with 10% isopropanol, washed in Hexafluoroisopropanol (HFIP) and lyophilized.

DRG bioassay for NGF

To test if the Nerve Growth Factor (NGF) encapsulated within the alginate microspheres remains bioactive, Dorsal Root Ganglions (DRG) extracted from neonatal

rats were placed into poly-L-lysine coated wells in a 48 well plate. Following rehydration in culture media, alginate microspheres with NGF were placed into Transwell inserts. These inserts were placed into wells containing the DRGs. Alginate microspheres with Bovine Serum Albumin (BSA) were used to act as controls. Incubation media was composed of Eagle's minimum essential medium with glutamine supplemented with 10% glucose and 5% Fetal Bovine Serum (FBS). Additional negative and positive controls were set up by incubating DRGs with media supplemented with and without NGF. This assay was performed with three times per animal with E16 DRG's from four different animals. To visualize the DRGs, the cultures were fixed with 4% paraformaldehyde and immunolabeled for beta-tubulin neuronal marker TuJ1 (Covance).

DRG bioassay for chABC

To test if chABC remained active following electrospinning, a strip bioassay was used. Aggrecan, a CSPG known to inhibit axonal growth was deposited in a strip lane onto a poly-L-lysine coated Thermanox coverslip. DRGs were pinned onto the coverslips between these aggregan lanes and placed into Petri dishes with DRG culture media. Matrices were electrospun such that chABC was incorporated. These matrices were placed into experimental petri dishes, while control petri dishes only contained BSA matrices. The assay was performed three times per animal with E16 rat DRG's from four different animals. To visualize the DRGs, the cultures were fixed in 4% paraformaldehyde and immunolabeled for the beta-tubulin neuronal marker TuJ1

(Covance).

Animal Procurement and treatment:

All animal work was done following a VCU IACUC approved protocol. All animals were obtained from Harlan Inc. The animals used in chapter 1 were 60 day +/- 5 day old female Long Evans Hooded rats. The animals used in chapter 2 were 100 day +/- 10 day old female Long Evans Hooded rats.

Surgical Procedure:

The rats were first anesthetized with 5.0% Isofluorane (AERANE) in a gas chamber and kept under for the duration of the surgery using a nose cone with 3.0% isofluorane. A rectal temperature probe will be placed and the animal put on a warming blanket. Aseptic conditions were made by shaving the back of the rat and washing the skin with betadyne. A dorsal midline incision was made through the skin to expose the muscles of the back. An additional two incisions were made in order to expose the spinous process of the vertebrae. Tissue spreaders were used to expand exposure and access to the vertebrae. The T8 vertebra was then confirmed via palpation of the back. Using rongeur's, a laminectomy was performed, removing the lamina, transverse processes and exposing the spinal cord. We then performed a transection of 3.5mm +/- 0.5mm of the spinal cord, and replaced the cord with a 4mm portion of our electrospun matrix. Following implantation, the muscular layers were closed with silk suture (Ethicon). The skin was stapled shut with mitchell staples (FST). Antibacterial cream

(Bacitril) was spread over the incision to prevent infection.

Post Operative Care:

Post surgical rats were placed on a heat pad and monitored until conscious, and given an injection of gentimycin (10mg/kg) and buprenorphine (0.5 mg/kg). Buprenorphine was administered every 12 hours for the first 48 hours. Following surgery, rats were given daily prophylactic injections of gentimycin for 7 days to prevent bacterial infection. The water was supplemented with acetaminophen (150mg/kg) for 3 days post operation. Urine was voided from the bladder by manual stimulation twice a day until the rats began to self micturate (urine volume measured at <2 ml/day). Urinary tract infections were diagnosed and treated with 5 day cycles of gentimycin.

Basso-Beattie-Bresnahan locomotor rating scale:

The BBB scale is a well-known animal behavioral test. The rats are assessed for hind limb locomotor skills and scored on a 21-point system, with 0 being complete hind limb paralysis and 21 being complete mobility (Table 1.1). This test rates parameters such as joint movements, weight support, limb coordination, and gait stability. Animals were evaluated pre-operatively for four minutes in an open field using this scale, to ensure they are free of motor deficits. To perform the test, animals are placed in an open field (large round tabletop with high barrier on edge) and allowed to ambulate to the degree they are able for a four minute period. The animals were evaluated bi-weekly

for the duration of the experiments (1-12 weeks).

Tissue Collection:

Rats were euthanized using a pentobarbitol agent Euthasol (150mg/kg) injected intraperitoneally to induce a general plane of anesthesia and perfused transcardially with 0.1 M phosphate-buffered saline (PBS) and fixed with either 4% paraformaldehyde for immunohistochemistry or a 4% paraformaldehyde and 1% gluteraldehyde mixture for electromicrography. Spinal cords were then dissected out and allowed to further fix in paraformaldehyde or paraformaldehyde/gluteraldehyde mixtures for 48 hours at 4° C. The Spinal cords were then transferred into a 30% sucrose solution for 24 hours at 4° C. 20µm thick longitudinal sections of the implantation and immediate bordering spinal cord sections were taken on a cryostat, with sections representing 100µm out of every 500µm through the cord.

Immunohistochemistry:

Several antibodies were used to identify the cell population in the injury site. Astrocytes, microglia, schwann cells, axons, and fibroblasts were identified with GFAP(1:1000), IBA-1(1:1000), S100(1:500), Smi31(1:1000), and Fibronectin (1:100) respectively. All sections were blocked with 4% normal goat serum, rinsed with PBS, incubated in primary antibody overnight at 4°C, rinsed with PBST, blocked again, and incubated for 2 hours with Alexa Fluor 488 or 568 fluorescent conjugated secondary antibodies (Invitrogen). Sections where then counter stained with 4',6-diamidino-2-

phenylindole (DAPI), and coverslipped with mounting medium (Vectashield). Smi31 antibody (Covance) for Neurofilament Heavy required a non-phosphorylated block and rinse, Tris Buffered Saline was used instead of Phosphate Buffered Saline.

Vasculature was identified in principle by the identification of Red Blood Cells (RBC). RBCs were identified by utilizing their native glutathione peroxidase activity. A DAB peroxidase mixture (0.05% DAB with 0.015% H2O2) was placed onto each section for variable time to allow visualization through brown crystalline precipitate. The use of immunohistochemistry in these experiments was to demonstrate the presence of cell populations and was not quantified.

Electron Microscopy:

For EM, the transection/implantation site was post-fixed in buffer glutaraldehyde and then in 1% OsO4 for 1hr, dehydrated through an ethanol series and infiltrated overnight in epon/araldite. 1µm "semithin" sections were obtained and stained with toluidine blue. Coronal thin sections were used to determine the diameter of monofilaments within the middle of the implant. Monofilament diameters were measured by taking 9 representative grids through the middle of the implant. Fibers were measured using a scale bar.

BBB Locomotor Rating Scale

0	No observable hind limb movement
1	Slight movement of one or two joints, usually the hip and/or knee
2	Extensive movement of one joint or extensive movement of one joint and slight movement of one other joint
3	Extensive movement of two joints
4	Slight movement of all three joints of the hind limb
5	Slight movement of two joints and extensive movement of the third
6	Extensive movement of two joints and slight movement of the third
7	Extensive movement of all three joints of the hind limb
8	Sweeping with no weight support or plantar placement of the paw with no weight support
9	Plantar placement of the paw with weight support in stance only (i.e., when stationary) or occasional, frequent, or consistent weight supported dorsal stepping and no plantar stepping
10	Occasional weight supported plantar steps, no forelimb-hind limb coordination
11	Frequent to consistent weight supported plantar steps and no forelimb-hind limb coordination
12	Frequent to consistent weight supported plantar steps and occasional forelimb-hind limb coordination
13	Frequent to consistent weight supported plantar steps and frequent forelimb-hind limb coordination
14	Consistent weight supported plantar steps, consistent forelimb-hind limb coordination; and predominant paw position during locomotion is rotated (internally or externally) when it makes initial contact with the surface as well as just before it is lifted off at the end of stance or frequent plantar stepping, consistent forelimb-hind limb coordination, and occasional dorsal stepping
15	Consistent plantar stepping and consistent forelimb-hind limb coordination; and no toe clearance or occasional toe clearance during forward limb advancement; predominant paw position is parallel to the body at initial contact
16	Consistent plantar stepping and consistent forelimb-hind limb coordination during gait; and toe clearance occurs frequently during forward limb advancement; predominant paw position is parallel at initial contact and rotated at lift off
17	Consistent plantar stepping and consistent forelimb-hind limb coordination during gait; and toe clearance occurs frequently during forward limb advancement; predominant paw position is parallel at initial contact and lift off
18	Consistent plantar stepping and consistent forelimb-hind limb coordination during gait; and toe clearance occurs consistently during forward limb advancement; predominant paw position is parallel at initial contact and rotated at lift off
19	Consistent plantar stepping and consistent forelimb-hind limb coordination during gait; and toe clearance occurs consistently during forward limb advancement; predominant paw position is parallel at initial contact and lift off; and tail is down part or all of the time
20	Consistent plantar stepping and consistent coordinated gait; consistent toe clearance; predominant paw position is parallel at initial contact and lift off; tail consistently up; and trunk instability
21	Consistent plantar stepping and coordinated gait, consistent toe clearance, predominant paw position is parallel throughout stance, consistent trunk stability, tail consistently up

Terms and Operational Definitions

Slight	partial joint movement through less than half the range of joint motion
Extensive	movement through more than half of the range of joint motion
Sweeping	rhythmic movement of hind limb in which all three joints are extended, then fully flex and extend again; animal is usually lying on its side, the plantar surface of paw may or may not contact the ground; no weight support across the hind limb is evident
No Weight Support	no contraction of the extensor muscles of the hind limb during plantar placement of the paw; or no elevation of the hindquarter
Weight Support	contraction of the extensor muscles of the hind limb during plantar placement of the paw, or elevation of the hindquarter
Plantar Stepping	paw is in plantar contact with weight support then the hind limb is advanced forward and plantar contact with weight support is reestablished
Dorsal Stepping	weight is supported through the dorsal surface of the paw at some point in the step cycle
forelimb-hind limb Coordination	for every forelimb step an hind limb step is taken and the hind limbs alternate
Occasional	less than or equal to half; <50%
Frequent	more than half but not always; 51-94%
Consistent	nearly always or always; 95-100%
Trunk Instability	lateral weight shifts that cause waddling from side to side or a partial collapse of the trunk

Table 1.1. The 21-point BBB locomotor scale used to rate functional recovery after SCI. (Chow, 2009)

Chapter 3

Exploring the Histology of Electrospun Implants *In Vivo*

Introduction

There exist a myriad of obstacles facing successful therapy to spinal cord injury. Following spinal cord injury, damaged axons are separated from their source of neurotrophic support, which results in additional cell death. At the gliotic scar surrounding the damaged tissue, neuroinhibitory compounds such as chondroitin sulfate proteoglycans are expressed which inhibit growth cones in regenerating axons. Finally, the formation of a fluid filled cyst represents a gap where axons have no substrate to grow on. In order to address these issues, we demonstrated the ability to create an implant using a process called airgap electrospinning with PDS as a substrate. Additionally, these implants were able to direct neurite outgrowth, contain bioactive neurotrophic factors and enzymes to reduce the activity of the neuroinhibitory compounds. This represented a novel combinatorial approach to spinal cord injury.

Nerve growth factor (NGF) is essential for the growth and survival of sensory neurons that project their axons through the dorsal columns (Acosta et al., 2001; Tusynski et al., 1994). For the first set of experiments, we used an airgap electrospun matrix made with PDS, and supplemented these with alginate microspheres containing NGF and chABC.

To test these matrices, we opted to use a complete transection model for SCI. While a complete transection rarely happens in the clinical setting, this model is

nonetheless the preferred model in the laboratory because the functional deficits are reproducible and recovery can be attributed to regeneration following injury rather than axon sparing.

While individuals suffering from spinal cord injury have a plethora of health problems extending beyond paralysis, motor function is perhaps the easiest deficit to visualize as well as score.

The BBB test is an open field locomotor test named after Basso, Beattie and Bresnahan that rates the quality of hindlimb movements (Basso et al., 1995). In this experiment, we used the BBB test to show animals with implants fortified with NGF and chABC scored better than those with only implants or no implants at all. While these animals showed functional recovery, these implants had never been given a histological examination. In this chapter, we analyzed tissue sections of rats given our spinal cord implant following a complete transection injury to gain greater understanding of how the implant's monofilaments interact with host tissues and cells. Axons were discovered within every segment of our implant. As every axon had been severed in our SCI model, we also examine the level of axon degradation rostral and caudal to the level of the injury to determine differences in axon tract survival. Finally, we discover the presence of functional vascular supply supporting the cellularization and axonal growth into the implant.

Results

The spinal cords and implants were very well integrated upon gross examination

following dissection, with all cords being extracted as one continuous object. While scar tissue was present, it was quite minimal and confined to the cord. Implants did vary in their sizes, a result of the electrospinning process forming an imperfect cylinder.

Monofilament interaction with the spinal cord:

The airgap electrospinning process had been shown to create fibers of approximately the same diameters with a densely packed formation (Figure 1.4). Fiber diameters were stated to be confined up to 3µm. However, upon examining the fibers at the EM level post implantation, we were able to show great variation in size of these fibers (Figure 3.2). Analysis of these fibers at the EM level show a variety of fibers of all sizes, measured up to a 60 fold difference in fiber size. The graph in Figure 3.2 weighs percentage of fibers to their diameter. A scattering of fiber sizes is prevalent throughout the implant, with over 60% of fibers having diameters 6 µm or lower. This does not prevent fibers from being spun at a much larger diameter, with the largest fiber diameter measured at 32 µm. Figures 3.2A, 3.2B, and 3.2C show three different fibers in the same section. All three images were taken with the same magnification to show the variability in fiber diameters. Figure 3.2A is centered on a fiber 2 µm in diameter, but below it are two other fibers that are approximately 1 and 0.5 µm in diameter. Figure 3.2B shows a fiber with a diameter of 10 µm, while Figure 3.2C shows a fiber measuring 25µm in diameter. These are representative images of monofilaments that can be found readily. Within the implant, monofilaments can be found in clusters that exhibit uneven spacing. No correlation exists between fiber diameter and location

within the implant. Using a cross section of the spinal cord at the rostral border with the implant, a distribution favoring the periphery of the spinal cord exists. These fibers can be seen in greater number in the peripheral white matter (figure 3.3). This section was taken in spinal cord, thus the gray and white matter can be clearly seen. Curiously, there are very few monofilaments seen in the gray matter. As cell mass is higher in the gray matter, it is possible that the cells infiltrated the matrix centrally, pushing monofilaments peripherally. With the greater abundance of cells in gray matter, it also stands to reason microglia and macrophages engulf the implant at the gray matter scaffold interface to a greater degree than at the white matter scaffold interface. Monofilament breakdown and degeneration occurs over time, however there is no consistent pattern to their degradation. In figure 3.4, fibers undergoing degradation are seen at both the LM and EM level. These fibers display degeneration from central to peripheral, as well as peripheral to central. Some fibers appear to crack and fragment into pieces whereas other fibers can be found within a larger space of geometric similarity to their current shape, suggesting a uniform degradation from the periphery inward. Larger fragments of monofilament may be engulfed by macrophages. At the EM level, figure 3.4 also displays the extent to which ECM is laid down surrounding the fibers. There is no space between fibers and host cells or ECM, indicating the electrospun PDS is highly biocompatible.

The cells infiltrate the matrix over time, and interact well with the electrospun fibers readily, as seen in Figure 3.5. Using DAPI to visualize nuclei, alignment of fibers in the implant affects cell infiltration. Figure 3.5A shows a portion of our electrospun

matrix that is highly aligned 3 weeks post implantation. Figure 3.5C is that portion of the matrix with DAPI applied, and cells are seen throughout the entire segment. Figure 3.5B shows a portion of the same matrix that has become unaligned. This nonalignment may have occurred during the spinning process. Utilizing DAPI, we can hardly see any cells within this unaligned segment (Figure 3.5D). This shows that misalignment of monofilaments during spinning may prevent cells from entering and disrupting the continuity of the cellularization within the matrix.

Axons:

Axons are found throughout the extent of the implant. Myelinated axons can be seen coursing through the middle of the matrix in figure 3.6. While no normal spinal cord architecture exists within the implant, it is encouraging that so many axons were found in the implant. This shows the implant has succeeded in its function for providing a substrate for axons to grow through. It is unknown if these axons are continuous to the other side because of the disruption from what appear to be fibroblasts.

Axon tracts above and below the lesion could be seen in differing levels of degradation. Figure 3.7 compares the dorsal column above and below the level of the lesion. The axon tracts are highly degraded rostral compared to caudal to the injury. Macrophages are seen at the arrows enhancing myelin debris cleanup. Figure 3.8 shows the reticulospinal tract, where many axons have been preserved quite well compared to the dorsal column, however a difference is seen rostral vs. caudal. In congruence to the

idea that axon tracts connected to their somas remain preserved better than the axons disconnected, the reticulospinal tract is in far better condition rostral to the lesion compared to caudal. Some tracts are degraded both above and below the level of the implant equally, suggesting differential survivability of axon tracts. This suggests that it may be essential to target axon tracts independent of one another.

Vascular supply:

The existence of a functional vascular network was discovered in the implants. This is important for long term glia and neuron survival through the implantation. It appears that endothelial cells associate themselves with monofilaments to help direct their growth. Figure 3.9C shows an EM level of an endothelial cell wrapped around a fiber. Many endothelial cells can be seen either wrapped around a monofilament, or with a monofilament within the lumen of a presumptive blood vessel. This may suggest that at one time this monofilament occupied the entire space of the lumen and degraded over time. While these endothelial cells can use monofilaments, there are many similar sized monofilaments without endothelial cells associated with them. It appears that endothelial cells tend to associate with monofilaments within a restricted range of diameter, however not all monofilaments at these sizes can be seen associating with endothelial cells. Figure 3.9D shows a fiber of similar size without an endothelial cell associated with it. To prove that these EM image are in fact of endothelial cells, Figure 3.9B shows blood supply within the matrix at the LM level. Biconcave RBCs can be seen within the lumen that still has 2 monofilaments inside. This shows that these

endothelial cells that are using these monofilament fibers as substrates for growth are doing so in a novel manner, and anastomosing to form functional blood supply within the implant.

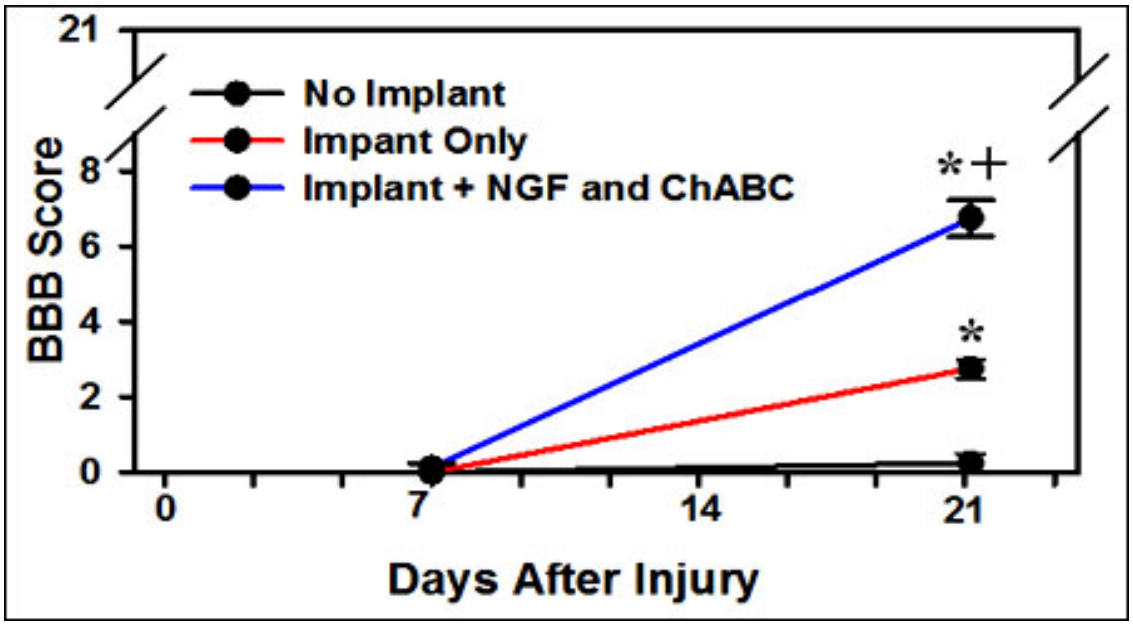

Figure 3.1. Recovery following surgery and implantation. BBB scores of experimental animals that were either given an electrospun implant containing NGF and chABC, an electrospun implant with alginate beads only, or no implant at all. 7 days post injury animals show little to no hindlimb movement. By 21 days, appreciable differences have emerged. Animals with no implant show no hindlimb movements. N=1, 3, 3 for no implant, implant, implant +NGF + ChABC.

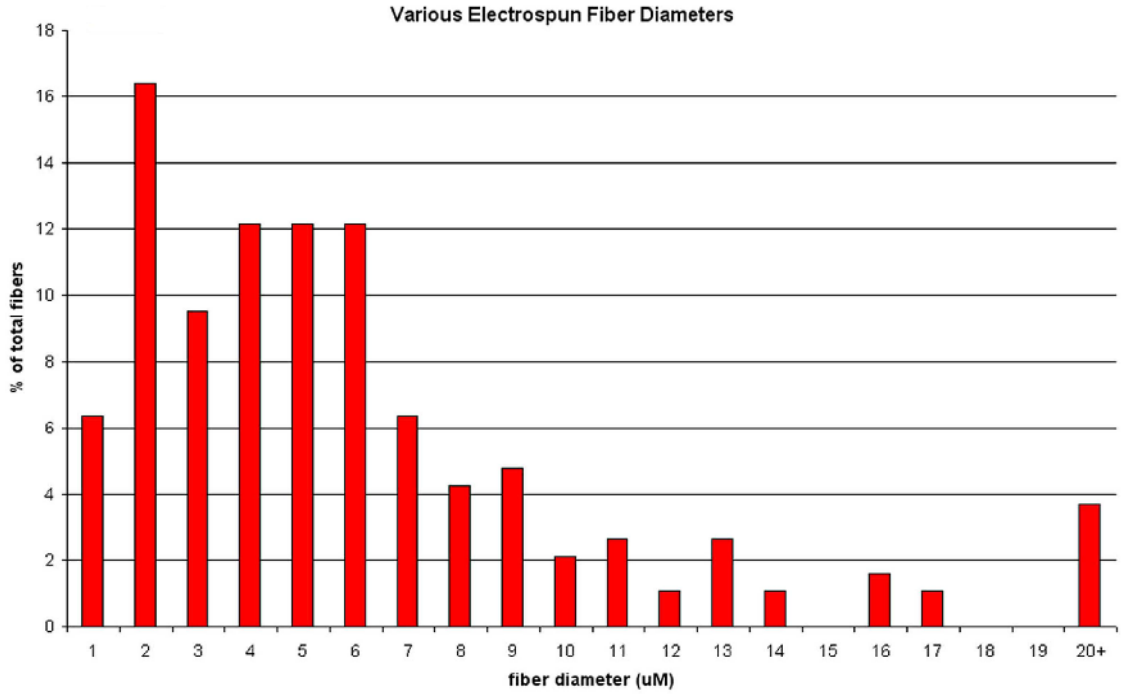

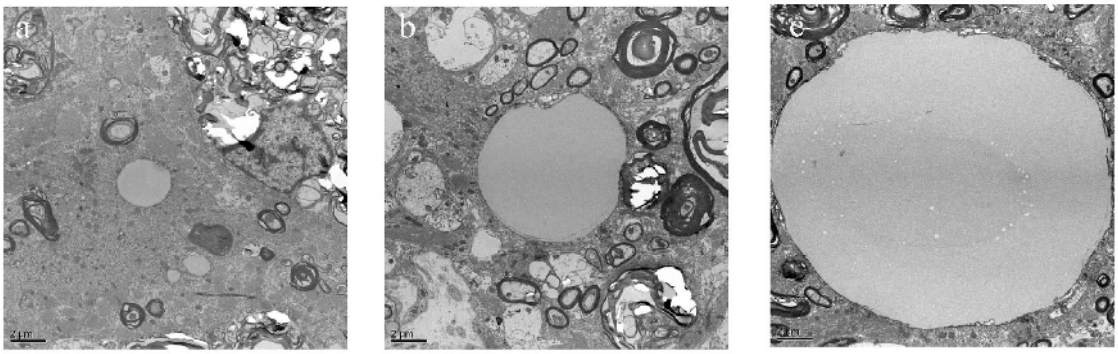

Figure 3.2. Electrospun monofilament diameters. The graph indicates % of total fibers in relation to their diameter when measured at the EM level using a scale bar. Representative sections were analyzed throughout the section, N=125 per section analyzed. Image (A), (B), and (C) are at the same magnification, demonstrating a high level of fiber size variability. (A) contains a monofilament of 2 µm diameter in the center, however below this monofilament are two smaller monofilaments with diameters as small as 0.5 µm. The monofilament in (C) is measured at 20 µm, which is the largest that could be fit at this magnification. Monofilaments were found up to 32 µm. (Scale bar = 2 µm)

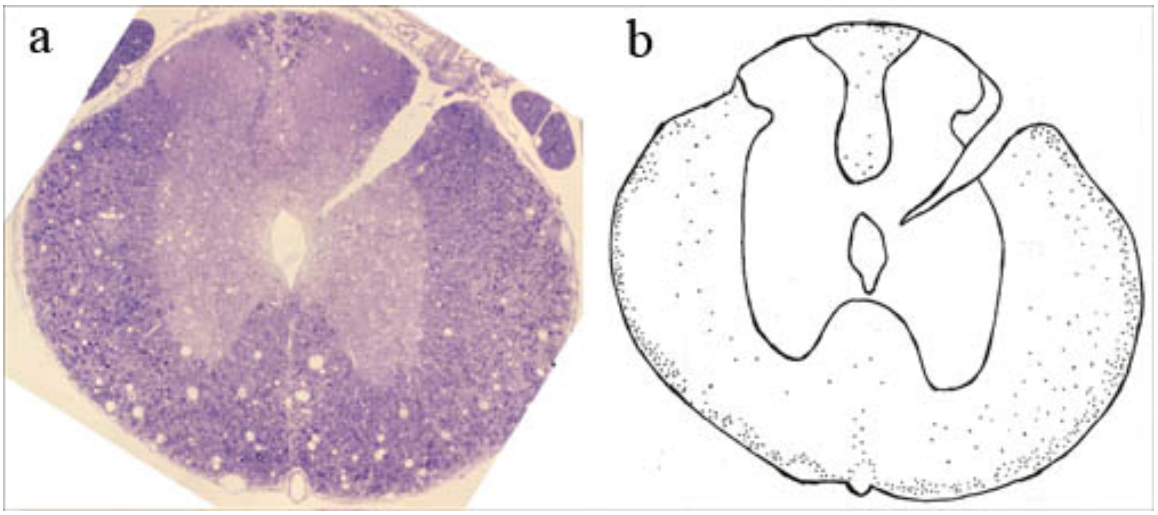

Figure 3.3. Electrospun monofilament distribution. (A) Cross section of the spinal cord immediately rostral to the implantation. Monofilaments can be seen throughout this segment of the spinal cord. (B) denotes every monofilament found in this section visible to the eye at 20x under LM. A distribution exists favoring the peripheral white matter. Note that at this level monofilaments with diameters less than 1 μm may not be visible to the eye.

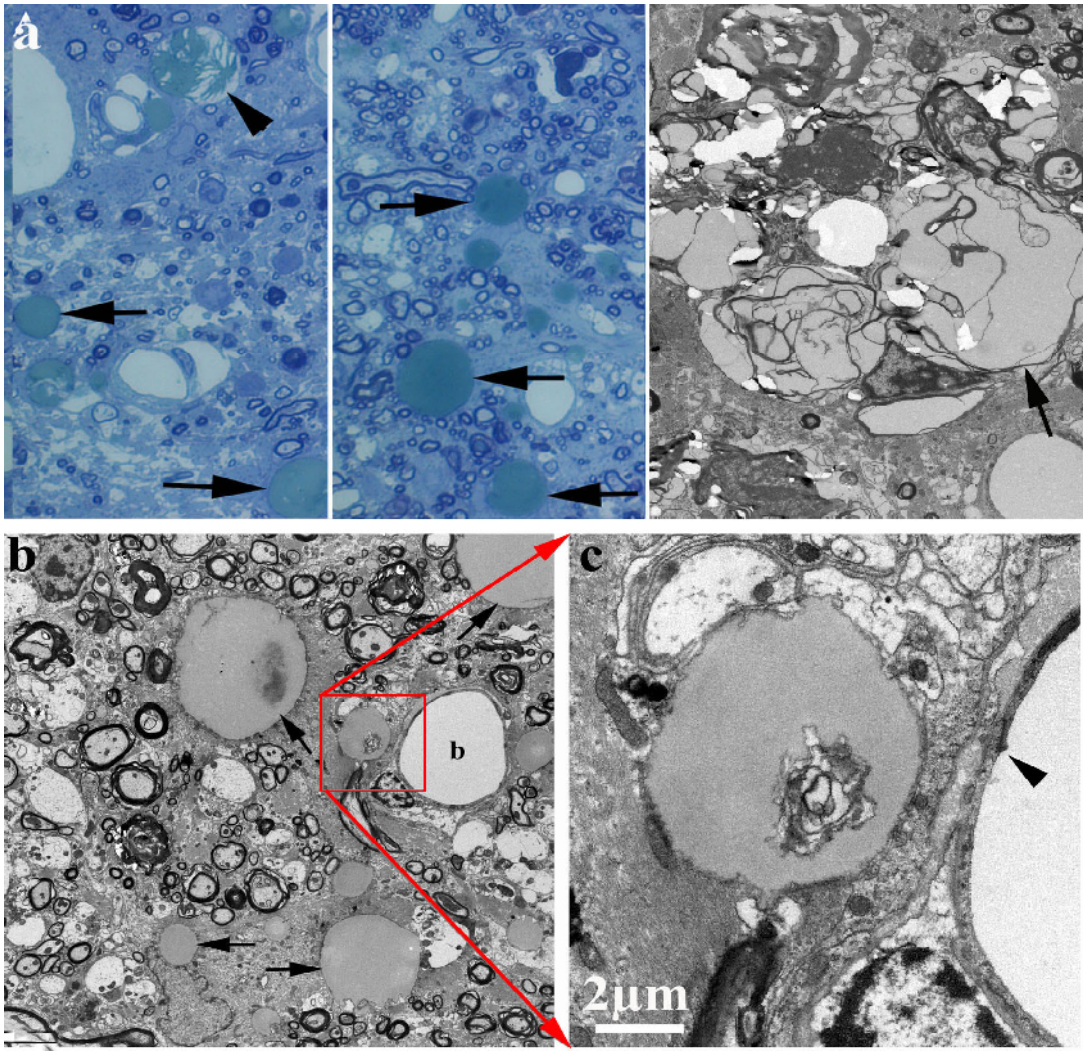

Figure 3.4. Monofilaments at varying levels of degradation. Monofilaments can be seen degrading at the (A) LM or (B and C) EM level. These monofilaments display a variety degenerative properties, and with no recognizable specificity. In image (A), neighboring monofilaments exhibit great levels of degradation, or no degradation at all. Degradation is occurring centrally as seen in image (C).

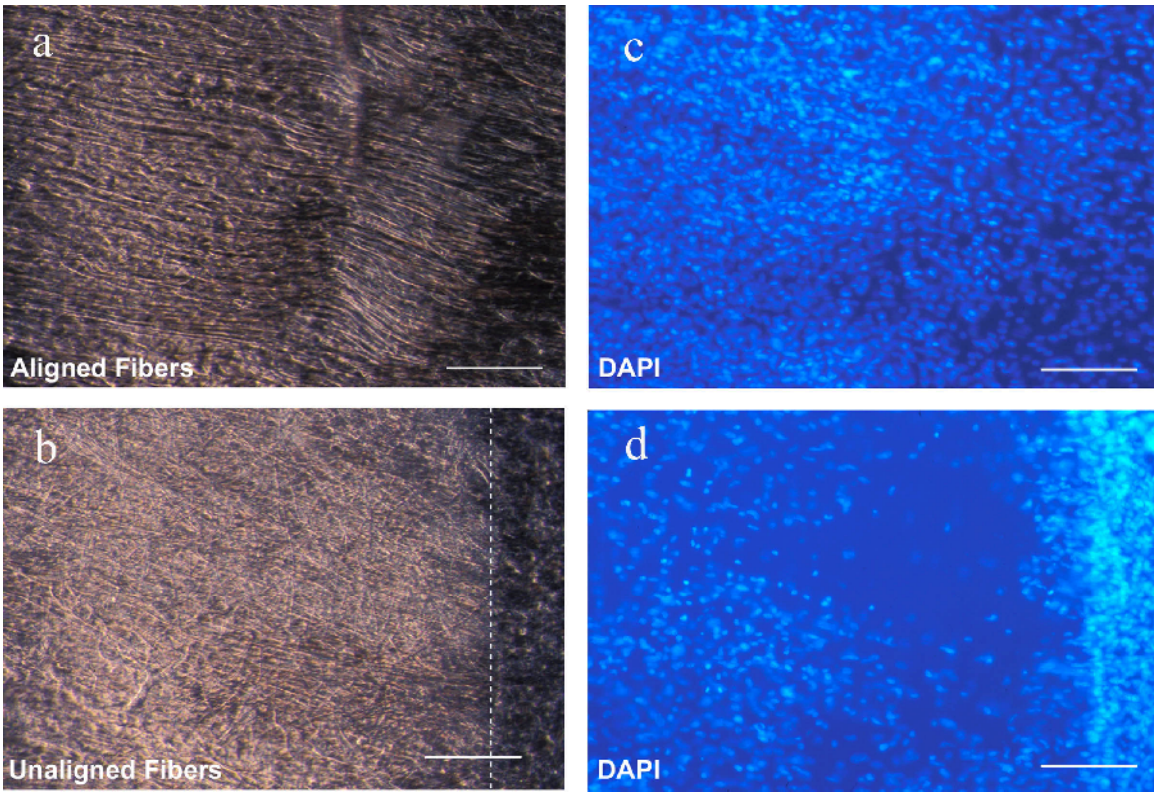

Figure 3.5. Aligned fibers affect cell infiltration. This image demonstrates the effect of alignment in the electrospun matrix has on cell infiltration. (A) and (B) are phase images of the alignment of a portion of the same implant. Within this implant, (A) is highly aligned, whereas (B) has is unaligned. Using DAPI, we can see the cell infiltration difference. Cells have infiltrated the extent of the aligned portion as seen in (C). However, cells can not enter the implant when the fibers are unaligned as seen in (D). Scale bar (A-D) = 100 um.

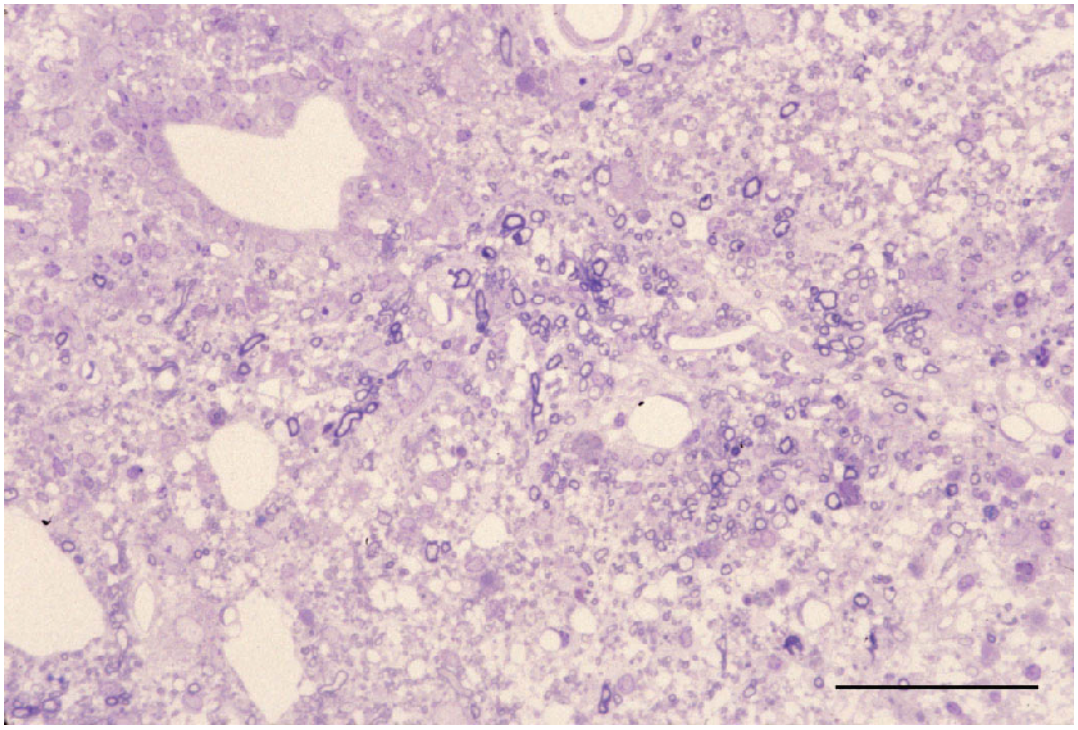

Figure 3.6. Cross section through center of implant. Axons can be seen at the LM level at 40x magnification in cross section through the middle of the implantation. This tissue is highly irregular. There appear to be many round empty spaces around the size of capillaries present in this image, however, these spaces do not contain endothelial cell bodies. These could represent the space in which monofilaments once resided. Of particular interest are unmyelinated axons found in this section of the implant. Scale bar = 100 um.

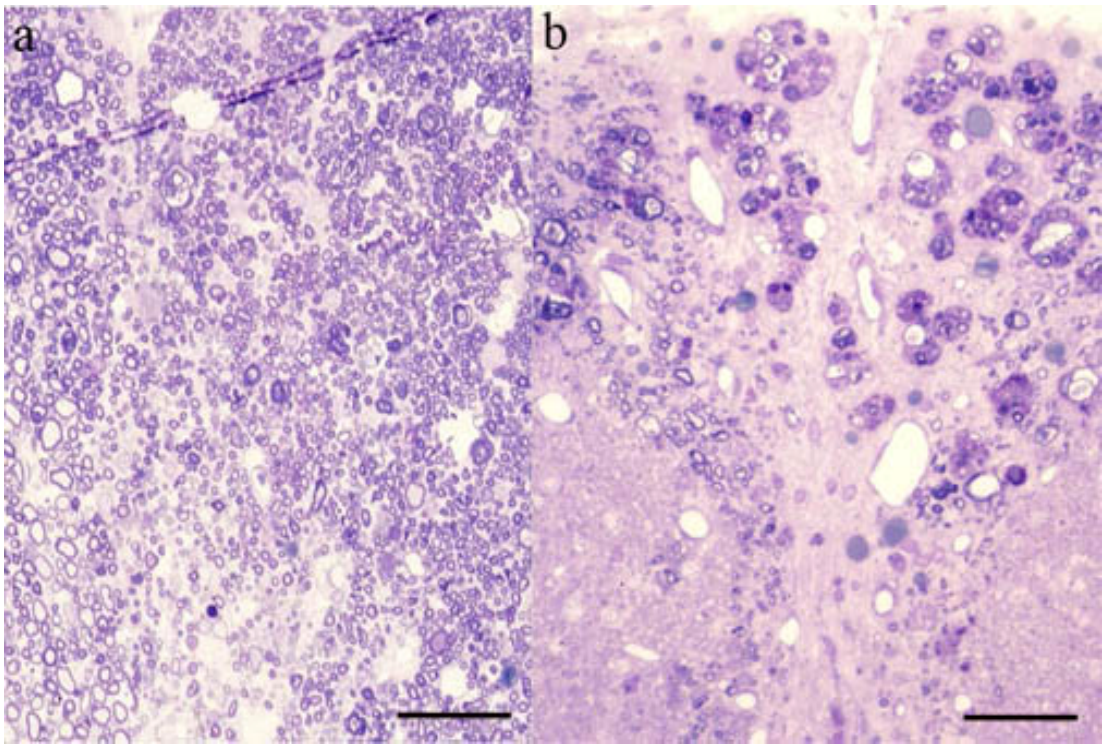

Figure 3.7. Comparison of the Gracile Fasciculus. This image depicts a comparison of the gracile fasciculus (A) caudal and (B) rostral to the level of the implant. Myelin degradation has occurred in both levels of the spinal cord, however a greater percentage of macrophages exist in the rostral cord. Very few myelinated axons can be seen in (B) whereas there are still plentiful myelinated axons is (A). Scale bar = 100 um.

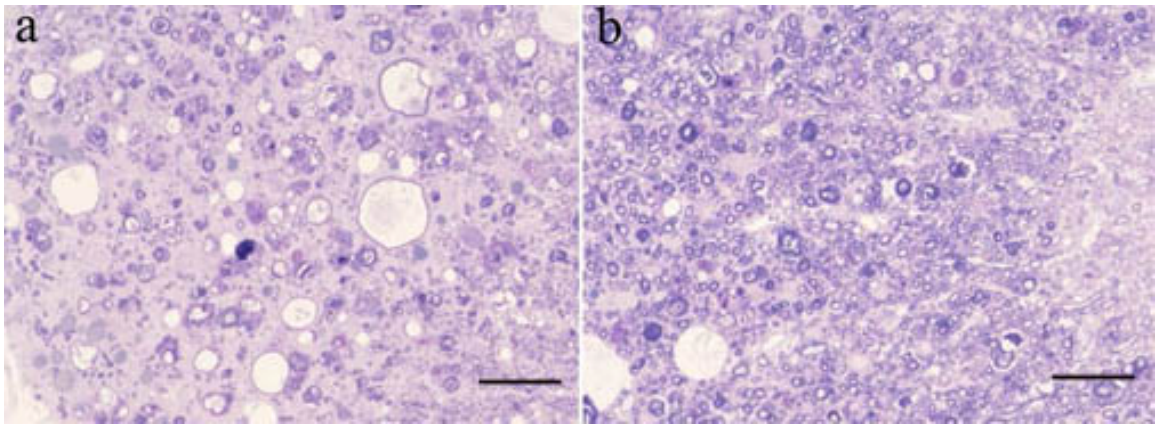

Figure 3.8. Comparison of the Reticulospinal tract. This image depicts a comparison of the Reticulospinal tract (A) Caudal and (B) Rostral at the light microscope level using 40x magnification. Similar to the dorsal column, the reticulospinal tract has undergone some level of degradation. Since the cell bodies of this axon tract originates in the reticular formation rostral to the injury, the axon tracts are predictably preserved greater in (B) than (A). Scale bar = 100 um.

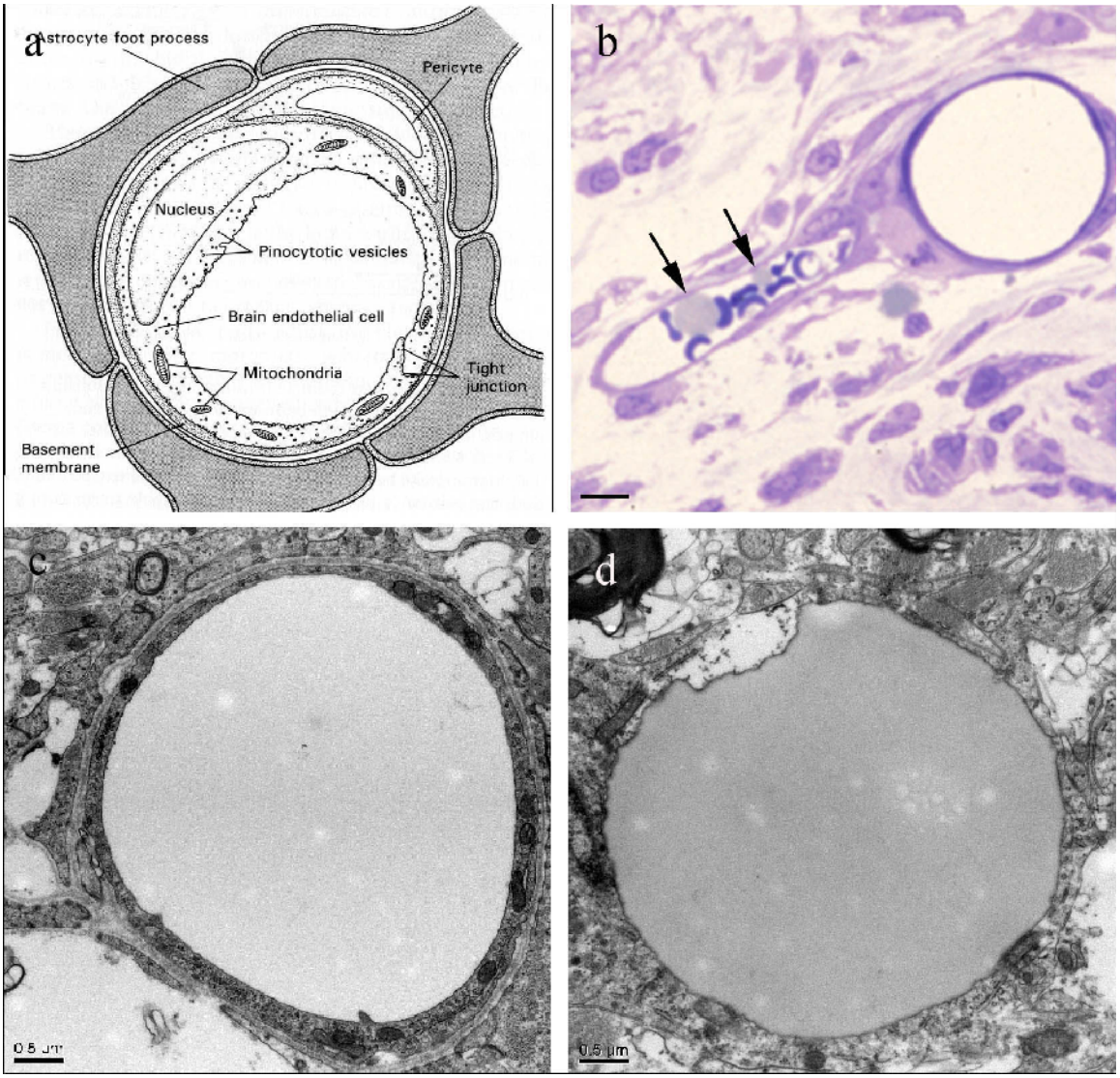

Figure 3.9. Endothelial cells wrap around monofilaments. Endothelial cells wrap themselves around monofilaments in the creation of new blood vessels. (A) is a cartoon of an endothelial cell and the astrocytic foot processes, the tight junctions represent the blood spinal cord barrier. Image (C) is an EM of an endothelial cell that has wrapped around a monofilament. There is no space between the monofilament and the cell body. Not all monofilaments of this size have endothelial cells associated with them. (D) is a monofilament without an endothelial cell associated with it. It can be seen degenerating from the periphery inward. (B) is a LM image depicting a blood vessel with arrows pointing at the monofilaments still in the blood vessel. RBCs can be seen in the lumen. Scale bar (B) = 10 um, (C and D) = 0.5 um.

Discussion

Spinal cord injury has many obstacles to successful regeneration including the fluid filled cyst, neuroinhibitory compounds and cell survival following axotomy. In this experiment, we addressed these obstacles by creating an electrospun matrix containing neurotrophic support that was implanted into completely transected rats. We sought to elucidate questions and concerns regarding the use of both electrospinning to create a spinal cord implant, and the use of a complete transection *in vivo*. With the help of an experience neurosurgeon, the mortality rate during the operation was less than 10%. Rats were capable of surviving 12 weeks post injury before being sacrificed for tissue collection. We showed that the fibers created during electrospinning were able to associate with the host tissue in a very seamless fashion. Perhaps of greater significance, we showed that axons grew through the implants. Finally, we were able to show that functional vascular supply was present in the implant.

One of the first observations we noted was that the fiber diameters were not uniform as predicted. Having fibers of different sizes may not be deleterious. While cells have had no trouble entering the scaffold, it is not known if a relationship exists between cell type and fiber diameter. Endothelial cells appear to utilize smaller diameter fibers by wrapping themselves around to create a vessel. The lumen becomes functional when the fiber degrades. It appears that capillaries formed by endothelial wrapping may come in unnatural sizes as the lumen of the newly formed blood vessel takes on the size of the original fiber. If these fibers become larger, rarely are there cells surrounding them. Within the implantation, there are no areas of empty space. Cells

and ECM have literally pressed right up against these fibers, showing beautiful integration of synthetic tissue with biological tissue. However, differing degradation rates make these spaces between fibers variable over time; this suggests that as fibers degrade, cells or ECM must take their place. This would be further beneficial as long term remodeling is taking place in the system. With fibers of different sizes, it is expected that the smaller fibers would degrade at different rates than the larger fibers, though we are unable to confirm this. In analyzing the matrix 12 weeks post injury and implantation, there are both small and large fibers in varying states of degradation. Due to our limited number of experimental animals processed for EM, it is unknown if the smaller fibers were larger at one time and degraded from the outside in at a constant rate, maintaining morphology. A chronicling of the matrix *in vivo* with varying time points would be necessary to understand the change in fiber distribution and diameter over time. That being said, it is peculiar that within spinal cord tissue removed from the injury, fibers can be found. In the section rostral to the transection, we clearly show the electrospun monofilaments present throughout both gray and white matter, but with a much greater distribution toward the peripheral edges of the spinal cord. It is possible that infiltration of cells begins from the gray matter where there is a greater abundance of cells, which in turn could cause the fibers to spread outward towards the periphery. Another possible explanation is that fibers degrade quicker centrally. We hypothesize that because these fibers extend into the spinal cord tissue, they may act as an anchor for cells to infiltrate the implant.

Cell infiltration is one of the necessary aspects for any spinal cord implant to be

successful. With the ultimate goal of axon regrowth, glia must be able to enter and survive in the implant. While fibers are typically electrospun in an aligned fashion, variables such as moisture in the atmosphere can affect the electric field and result in fiber misalignment. Damage associated with surgery may also crush or damage the alignment of the implants. This is to be taken into consideration for future experiments attempting to cellularize the implants prior to implantation. Our images show that within a single matrix, areas of alignment and nonalignment may be present. The cell infiltration greatly varies depending on this alignment. It is essential then, that these implants need quality control prior to their implantation, and extra care must be taken to prevent damage during surgery. Mechanical damage to the implant during or prior to surgery can cause breaches in the fibers and cells to infiltrate from outside the CNS. This is especially troubling due to the fact that the meninges in our SCI model are completely removed along with the spinal cord. It was observed that axons running through the implant eventually may have met a scar of mesenchymal origin through a segment of the implant that may have suffered from crushing or infolding, which disrupted axons from traveling directly through. This brings the potential for cells to enter the matrix that enter from the dorsal/ventral aspect of the implant, rather than from the rostral or caudal edges where we design entrance to occur. By having all the fibers aligned, it stands to reason that axons entering one end would be directed straight through the implant without excessive diversions or branchings. Having compartmentalized aligned fibers may be the next step following axon regeneration, in order to maintain spinal cord architecture through the matrix.

Axon tracts above and below the transection have differing levels of degradation. Wallerian degradation is a process that occurs following neurotrophic support being removed from axon somas. If the baseline level of neurotrophic support is removed from the neuron, it may undergo programmed cell death. If this occurs, the myelin begins to degrade and fragment releasing neurite inhibitory debris. Axon tracts that are no longer associated with a cell body also undergo this degradation, albeit on a faster timeline. As this was a complete transection model of SCI, all neurons coursing through the T8-T10 spinal cord were axotomized. One would expect all axon tracts to have undergone devastating degradation 3 months post injury. While we subsequently observe that in fact all tracts had undergone degradation, we were able to see very distinct differences in amount of degradation suffered by each tract. This is an interesting discovery, as this could prove some axon tracts are hardier then others following significant injury. As the spinal cord is composed of both efferent and afferent neurons, it is essential to consider where the cell body is relative to its white matter tract. For example, the dorsal column gracile fasciculus has cell bodies caudal to the lesion. Understandably, the gracile fasciculus caudal to the lesion appears to be very well preserved, whereas the gracile fasciculus rostral to the lesion has undergone complete degeneration. Not all tracts exhibit such predictable behavior, for example, the rubrospinal tract exhibits similar degradation both rostral and caudal to the transection. This is particularly applicable in the short term, where rescuing an axon tract and having it reconnect to the distal end of the implant has yet to be accomplished. By understanding which tracts maintain their structure and exhibit greater potential for

regeneration, we can direct our efforts one tract at a time, which is something that researchers are only beginning to explore.

It is important to remember that while axons receive the most attention from researchers, vascular support is equally important. Following a spinal cord injury, hemorrhage and inflammation occur. While inflammation has often been made out to be a villain in spinal cord injury (Hirschberg et al., 1994; Blight, 1985), there is evidence that they may also be integral to neural regeneration (Lu and Richardson, 1991; Perry and Brown, 1992). Due to the loss of vasculature, angiogenesis occurs in response to the localized tissue hypoxia. Our experiments have resulted in the formation of blood vessels in great numbers throughout our implants. We believe this is because the endothelial cells are able to quickly migrate throughout the extent of the matrix by following the aligned fibers. It is controversial whether angiogenesis is beneficial or detrimental (Zhang and Guth, 1997; Wamil et al., 1998; Han et al., 2010), however the point is irrelevant if new tissue is going to exist at the original site of injury. The formation of new blood vessels in our implants is a step forward in the creation of a permissible environment for axons to occupy in place of the fluid filled cyst.

While we have shown great promise with the use of these electrospun implants, there are issues that need to be addressed. In order to maintain proper orientation of axon tracts throughout the implant, there must be no disruption of fiber alignment anywhere in the implant. When the electrospinning process takes place, these matrices that are created are handled frequently in order to perfect the shape, as well as to cut the

matrix into an appropriate length for implantation. Much of the mechanical damage can be prevented with experience and awareness; however there may also be modifications that can be made within the implant engineering.

Chapter 4

Improving the bridge

Introduction

Spinal cord injuries have shown increasing promise with the use of combinatorial strategies. An issue that all researchers dealing with contusion/cavitation type spinal cord injuries is endpoint formation of a fluid filled cyst. Axons require substrates to grow on, and thus a bridging material is required. In our lab, we use PDS as our substrate to create a bridge for axons to grow. Using airgap electrospinning, we are able to create a bridge that matches the shape of the spinal cord, while providing highly aligned fibers that have been shown to direct neurite outgrowth. This electrospun matrix can be enhanced with growth factors encapsulated within alginate microspheres, as well as other bioactive compounds that are beneficial to regenerating axons. Previously, the use of such bridges had shown a promising future, as axons, cells, and vascular supply were found within the implant. Areas of cell infiltration from the dorsal and ventral aspect of the implant seemed to create a segment of the implant where axons could not traverse. Additionally, it was seen that fiber alignment played a critical role in allowing cells to infiltrate deep into the implant. In an effort to enhance the electrospun implant, we devised a method to provide an electrospun coating using an alternate copolymer PGLA to direct cell infiltration from only the rostral and caudal aspect, while preventing cell infiltration from the dorsal or ventral aspect. This

copolymer had great success in preventing fibroblastic infiltration into the implant in peripheral nervous system (Telemeco et al., 2005). Figure 4.1 shows an implant within muscle tissue, with fibroblasts forming a capsule around PGLA copolymers. There is no fibroblastic infiltration into the core of the implant. Animals who receive complete transectional spinal cord injuries exhibit total paralysis of hind limbs. This demonstrates that the transection was in fact complete. In the weeks following injury, BBB scores typically rise if any regeneration is occurring. In this experiment we experienced little to no functional recovery as measured by the BBB scores (results not shown). Animals in this experiment were examined for axon regeneration, cellularization and vascular supply throughout the implants at 3 or 5 weeks post surgery. Following tissue collection, immunolabeling of Neurofilament Heavy within these animals showed that these axons were actually diverging away from the implants due to the presence of a mesenchymal scar. As the goal of this experiment was to further facilitate the axonal regeneration through our implant, this was an unfortunate turn of events. Regardless, while axons were unable to get into our implants, cells and vascular supply had no trouble entering the implant. In this chapter we attempt to understand to a greater degree monofilament interactions post implantation, hypothesize explanations for axon divergence, and document the creation of a vascular supply.

Results

Animals showed little to no signs of regeneration up to 5 weeks survival time. Upon dissecting the spinal cords from the bony canals, it was evident that massive scar

tissue was present. A previous experiment utilizing the same injury model resulting in enhanced functional recovery displayed spinal cords that were very well integrated with the implants. The spinal cords in this experiment were adhered to the lamina on many occasions, with several spinal cords unable to be removed in one continuous piece. Gross examination revealed what appeared to be the presence of blood vessels on the surface of the implant, which was later confirmed at both the LM and EM levels.

Monofilaments:

Monofilaments were present in the implant as expected, however the number of fibers was tremendously scarce compared to expectations. Since these animals had only survived up to 5 weeks post surgery, it was of particular interest to see so little monofilaments present in the implant itself. Large gaps in the implants were immediately visible, with spaces between cells and ECM. These gaps could represent a rate of degradation that was previously underestimated, but it is more likely an artifact created during tissue processing for EM. Further evidence is shown in figure 4.2, which appears to be a preserved cast of what the implant looked like prior to processing. While it is uncertain exactly how this preservation took place, monofilaments can be seen within perfectly round spaces, in a distribution resembling that of the SEM taken when first designing the implant.

Also evident in these sections was the presence of macrophages engulfing monofilament debris. Figure 4.7A is an example of endothelial cells wrapping around monofilaments, however this image also depicts an area of the implant where

macrophages are present and clearing out degrading monofilaments.

Axons:

Smi31 (Covance) was used to visualize Neurofilament H, a marker for mature axons. In figure 4.3, axons fluorescing in red can be seen diverging away from the electrospun fibers on the right. This shows that neuroregeneration taking place, as any axons shown curving away from the implant has done so as a result of neurite growth cones meeting a neuroinhibitory substance and redirecting the subsequent elongation of the axon. This was a common occurrence to all animals. Cross sections taken through the implant further revealed the absence of any axons in the implant.

To understand why these axons could not penetrate into the implant, we used immunostaining to gain insight into what cell population was responsible for this inhibition. Generally, a glial scar is often the component of neurite inhibition that repels axons from the injury site. To combat this, our electrospun implants contained chABC, which should have reduced the inhibitory activity of the compound CSPG that is released from the astrocytes making up the glial scar. Further proof that the glial scar was not responsible for this neuroinhibition was shown when we used a GFAP antibody to show no astrocytes present in the scar tissue immediately surrounding the implant (Figure 4.4A). However, by counterstaining with DAPI, we demonstrated that the tissue surrounding the implant displayed massive cellularization (Figure 4.4C). Thus the glial scar does not comprise the area responsible for neuroinhibition. Figure 4.5 is a 20x image of the scar tissue using a fibronectin (sigma) antibody. It appears as if

fibronectin (a marker for fibroblasts) exists within this scar tissue, suggesting that this scar is of mesenchymal origin.

Vascular supply

Despite the lack of axons growing through the implant, the PGLA capsule had no discernible effect on vascular entry. Figure 4.6 shows RBCs throughout the extent of the implant at 5 weeks post injury. These indicate in principle, the existence of capillaries and a vascular supply. Cells are clearly seen throughout all matrices implanted in animals regardless of PGLA capsule.

The evolution of a functional blood vessel within the matrix can clearly be seen at differing levels of formation. Figure 4.7 shows blood vessels at varying stages of formation and functionality. In 4.7A, an endothelial cell has wrapped the monofilament, which occupies the entire lumen. This blood vessel is not functional as the endothelial sprouting has likely not formed a loop for blood to flow. In 4.7B, the monofilament within the lumen of the endothelial cell is not occupying the entire area. This may be due to degradation of the monofilament. In 4.7C two monofilaments are seen within a single lumen. This may be a case where monofilaments are spun in a clump of fibers, such that a single endothelial cell could wrap two fibers simultaneously. In 4.7D, the appearance of a RBC signifies a functional blood vessel. The monofilament is seen within the lumen yet again, however is much smaller than the lumen. In 4.7E, multiple monofilaments are seen within the lumen, but even more relevant is the multiple RBCs that are present in the lumen. Quite a bit of blood flow is

coursing through this blood vessel considering the lumen diameter. Finally 4.7F is similar to 4.7E, however the tissue surrounding the endothelial cells are dramatically different. Looking closely at 4.7F, there appears to be another area where a cast of the monofilaments can be seen. Fibers with this type of distribution may have made up the entire empty space seen in this image prior to processing.

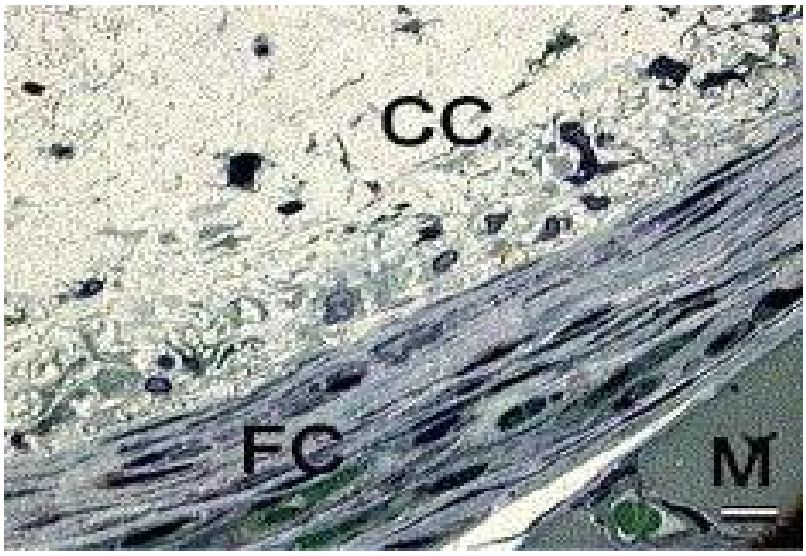

Figure 4.1. PLGA copolymer prevents fibroblastic infiltration when implanted intramuscularly. This image depicts the use of a PGLA copolymer in a dermal implant. The PGLA copolymer coating surrounded the core of the implant; fibroblasts were unable to penetrate this PGLA copolymer and instead formed a fibrotic capsule. FC = fibroblastic capsule, CC = core of the implant, M = endogenous muscle. Scale bar = 5 um. (Adapted from Telemeco et al, 2005)

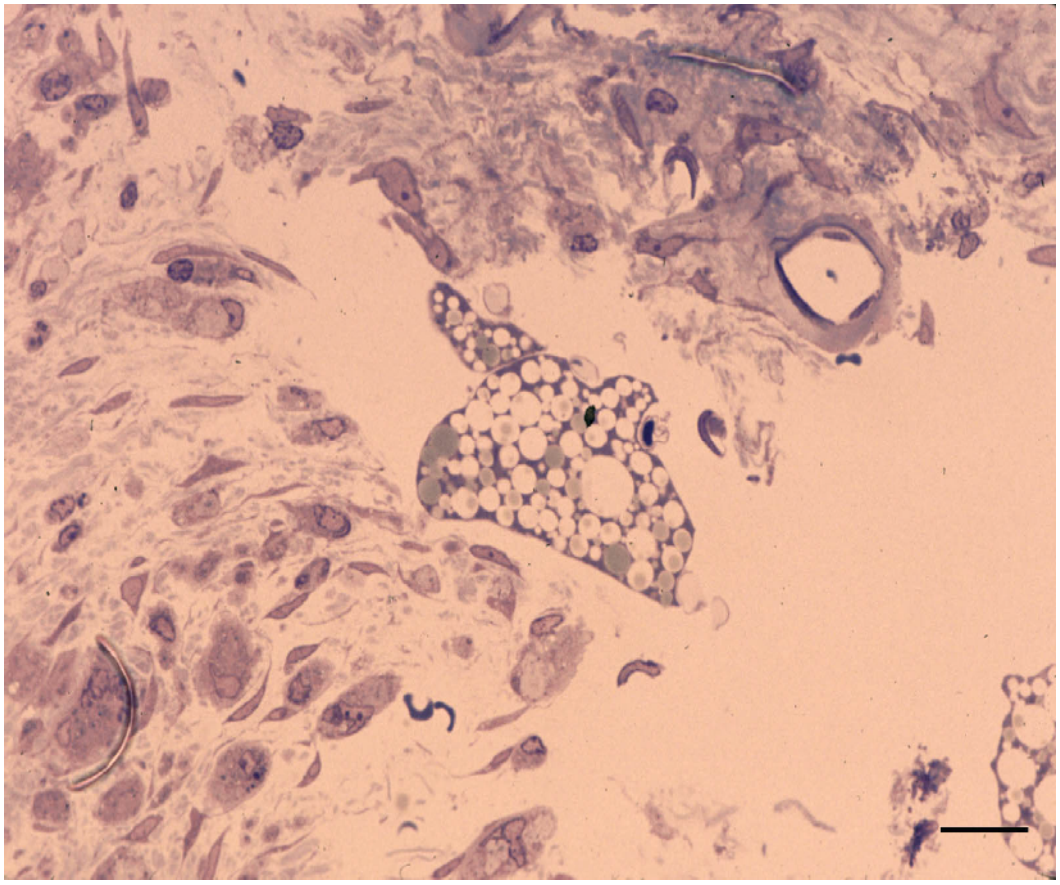

Figure 4.2. Preservation of monofilaments through processing. An image through the implant taken at 40x. This animal was given a complete transection and allowed to survive 3 weeks post surgery. Large spaces within the implant were found which were not present upon gross examination during dissection. This demonstrates a level of artifact previously undocumented. The tissue processing required for EM greatly degrades many of the monofilaments. Preserved within this image is a cast of what appears to be the packing density of the monofilaments prior to tissue processing. It more closely reflects what is expected of our matrices when spun. Scale bar = 20 um.

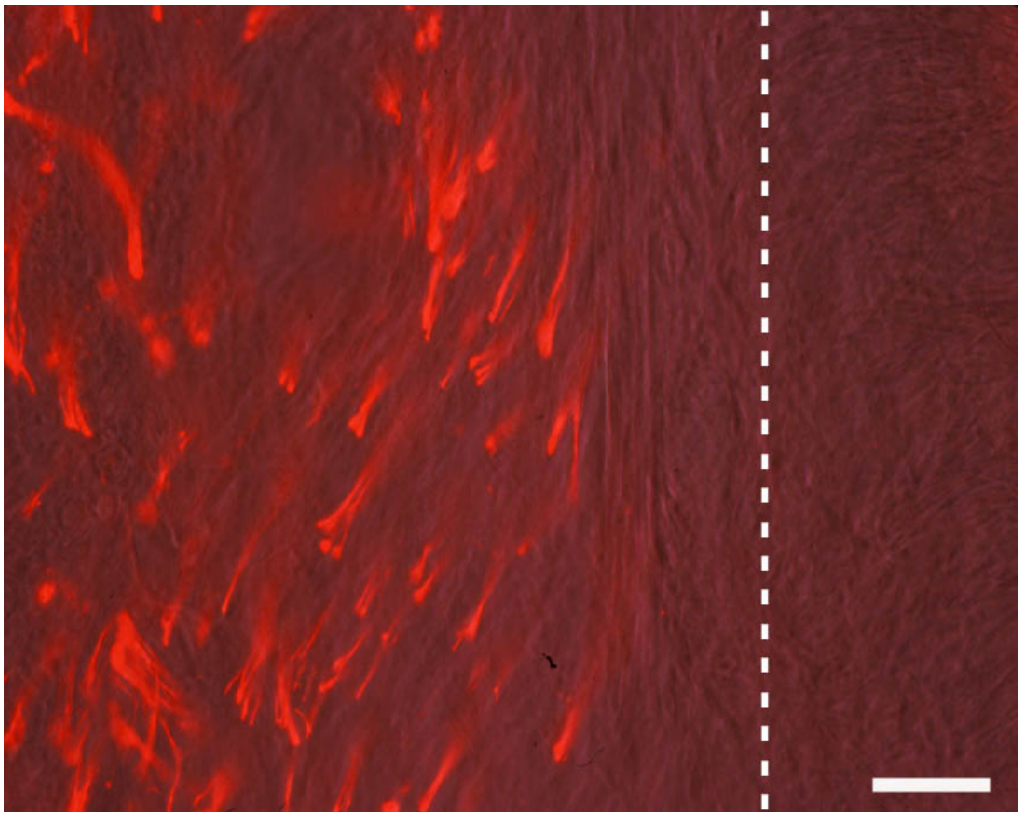

Figure 4.3. Axons at the tissue implant interface. Regenerating axons are seen in this image longitudinally at the spinal cord – implant interface. Post surgery, all axons are transected and would be visualized longitudinally. All axons seen in cross section are thus actively attempting to extend through the implant but unable to for unknown reasons. Axons were immunolabeled for Neurofilament heavy chain. Scale bar = 20 um.

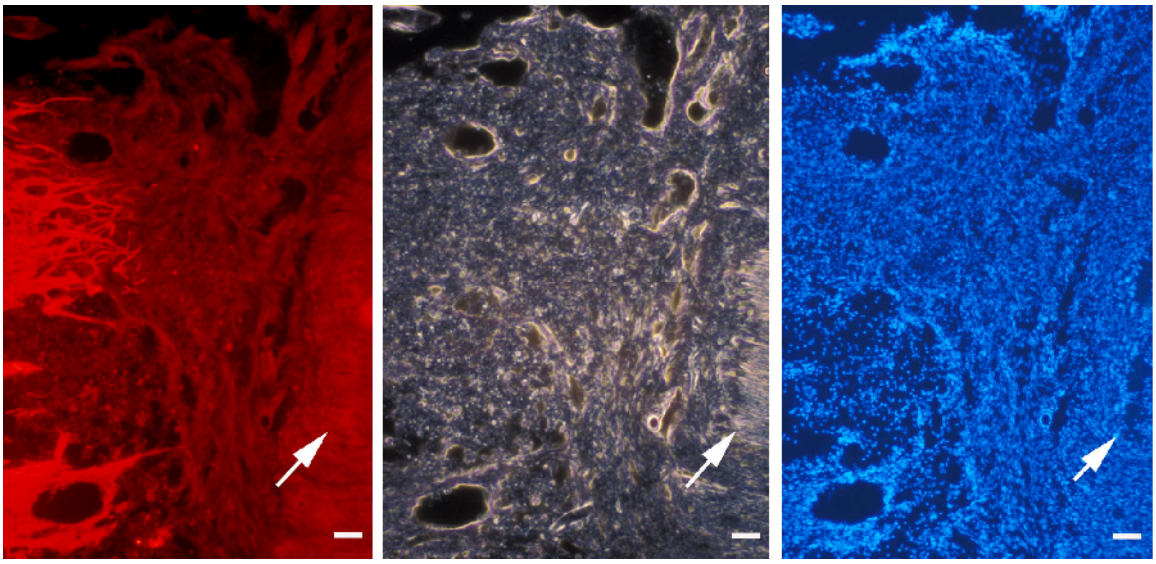

Figure 4.4. Scar tissue at the tissue-implant-interface. The field of view in these three images is identical. The arrow denotes the edge of our implant, where aligned electrospun fibers can be seen. The left side represents spinal cord and scar tissue. (A) This image was immunostained for GFAP astrocytic marker and visualized with an FITC conjugated secondary antibody. Astrocytes are clearly seen in an extremely condensed manner on the left. A gap of scar tissue remains separated from the astrocytes and implant. (B) This is a phase image showing the aligned fibers of the implant. (C) This is the same section with DAPI applied. Cells are seen in the space between astrocytes and implant. Scale bar = 40 um.

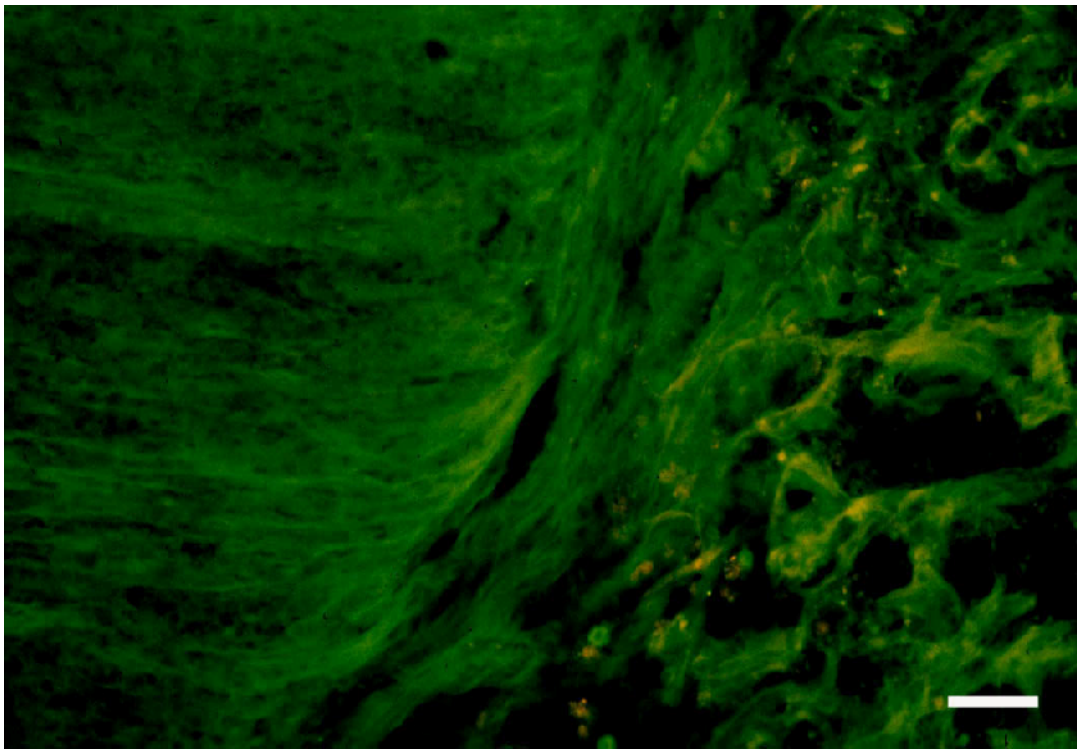

Figure 4.5. Fibroblasts at the tissue-implant-interface. This image was taken at 20x at the border of electrospun implant and spinal cord. The image contains scar tissue on the right and the aligned fibers on the left. This scar tissue may be responsible for the axon divergence. The section was immunolabeled against fibronectin, which is produced in fibroblasts. Fibronectin can be seen in the scar tissue as well as in the edge of the implant, demonstrating the likelihood that this scar is not derived from cells native to the CNS. Scale bar = 40 um.

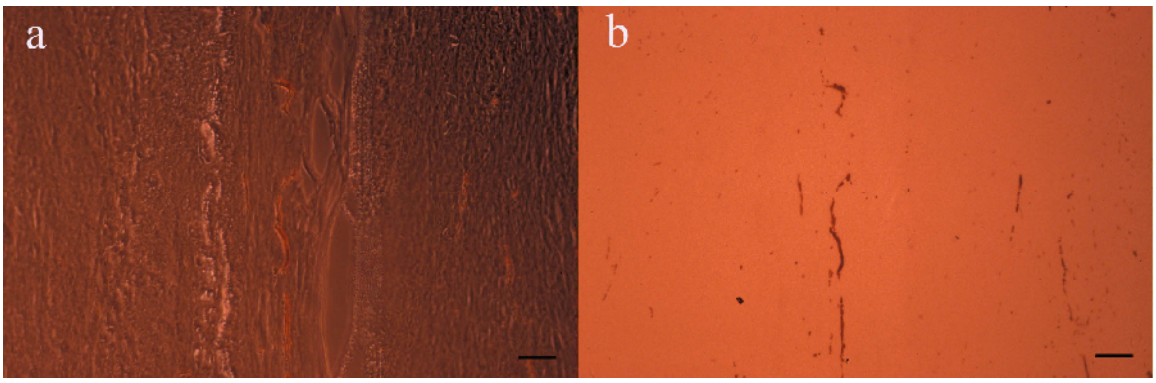

Figure 4.6. RBCs in the implant. Our implants show convincing evidence for vascularization. This image was taken at 4x of the electrospun matrix 3 weeks post injury. The aligned fibers can be seen in (A), with what appear to be tubes within. Utilizing the intrinsic glutathion peroxidase activity of RBCs, DAB+Peroxide was used to visualize RBC. These RBCs (Brown) display tremendous linearity and can be seen within the lumen of these blood vessels throughout the implant. Scale bar = 200 um.

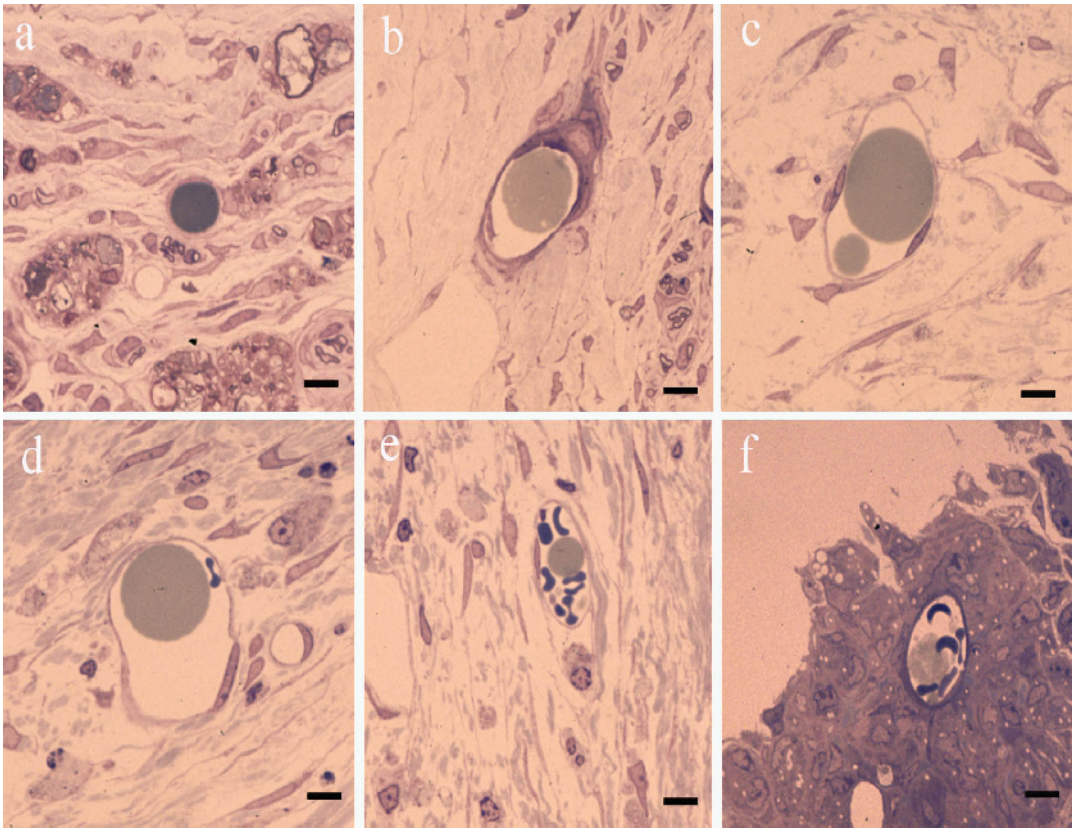

Figure 4.7. Generation of a functional blood supply within the implant. Endothelial cells wrap their cell bodies around these monofilaments and are able to grow long distances. The blood vessels become functional when these vessels sprout off the monofilament and connect with other endothelial cells to form loops. In (A), a monofilament occupies the entire lumen of an endothelial cell. The lumen is formed as the monofilaments degrade (B). Multiple monofilaments may be utilized to form larger blood vessels (C). When these endothelial cells undergo anastomosis, they become functional blood vessels. This process does not require a monofilament to have fully degraded as seen in images (D), (E) and (F). RBCs and monofilaments are present in the lumen of these endothelial cells simultaneously. Scale bar = 20 um.

Discussion

The use of combinatorial strategies addresses many obstacles facing SCI today. No current therapy exists that can address all obstacles simultaneously. Furthermore, differences in spinal cord injury models are not easily overlooked. The design of these matrices was to fill a physical gap created by a fluid filled cyst, the endpoint for contusional SCI. By switching to a transection model, we breach the meninges and allow massive infiltration of cell types that do not normally exist within the CNS. This is a problem that we must overcome if we are to use the complete transection model. The hypothesized use of a PGLA capsule was one such attempt at keeping fibroblasts from entering the implant. In contrast to expectations, in this experiment it did not create a fibrotic capsule limited to the implant. It is convincing that the underlying mechanism explaining the images of axons repelled prior to reaching our implant are in fact due to a mesenchymal scar created by fibroblasts. A possible explanation for this may be that the PGLA capsule caused greater irritation within the system, and thus increased fibroblast attraction. The PGLA degradation may have decreased the pH and affected fibroblastic attraction as well. Another possible explanation is increased inflammation due to surgical damage. The surgical procedure, specifically, the amount of tissue damage sustained during the surgery is a variable that is difficult to quantify. This damage compounds the existing individual variability between rats used as test subjects. Due to the fact that this experiment was performed by a less experienced surgeon, it is plausible that this fibroblastic infiltration will reduce as the surgeon gains experience. Regardless, the transection model should be performed in a manner as to

leave the dura mater as unharmed as possible.

In principle, increased activated microglia and proliferation of macrophages should come hand in hand with the induction of a greater inflammatory response. While inflammation is a necessary step in wound healing, many of these inflammatory cells may also release factors such as Fibroblastic Growth Factor (Tidball, 1995), enhancing proliferation and migration of fibroblasts to the wound site.

While there is no image provided in this dissertation, many sections were immunolabeled with iba-1, ionizing calcium binding adaptor molecule 1, which is specifically expressed in activated macrophages and microglia. The experimental animals showed a great deal of microglia activation and proliferation up to 5-6 mm away from the site of injury, which may suggest that the cord was irritated or stretched during surgery. Future experiments should continue to monitor microglial activation and proliferation away from the site of injury, perhaps this may be used as an indicator for surgical success beyond the generic loss of motor function.

The future usage of this PGLA coating is highly unlikely as previous experiments without the use of PGLA have shown axon penetration into the implant. The idea of creating a barrier to prevent unwanted cell infiltration is still relevant. Cell type repulsion may also be used to ensure fibroblasts do not enter the implant. It has been shown that astrocytes and non CNS cell types do not intermix harmoniously (Behzadian et al., 1995; Wilby et al., 1999). By seeding the implant with astrocytes prior to implantation, we may very well remove unwanted cell populations from entering.

Cell proliferation is evident soon after implantation and is dependent on alignment of the monofilaments. Having areas where the electrospun fibers are unaligned may compromise the continuity of any axon that enters the implant. Cells were unable to enter in areas of non alignment. Despite these areas that lacked cells, most implants contained a density of cells far greater than cord parenchyma. It was observed that endothelial cells wrap around monofilaments to form functional blood vessels. Endothelial cells prefer to grow on substrates, and it is likely that having monofilaments of all different sizes facilitate endothelial cell proliferation and blood supply formation. While many vessels contain degrading monofilaments within their lumen, most do not. From this histological viewpoint, it is impossible to tell if at one time they had monofilaments, because monofilaments appear to degrade at different time points. Therefore, it is unknown to what extent endothelial cells prefer the use of a monofilament. The appearance of a vascular network this quickly in the injury timeline may be beneficial for clearing of debris and nutrient delivery. However, since the blood spinal cord barrier has yet to be established, this also provides a direct route for additional inflammatory, immune and fibroblastic cells to gain entry to the injury site. While the establishment of a blood supply is essential in the grand scheme of restoring complete function in the injured spinal cord, evidence has shown angiogenesis can be both harmful and beneficial for spinal cord injuries. As pioneering blood vessels have the capacity to influence axonal guidance (Rosenstein and Krum, 2004; Zhang et al., 2009), the ability to entice endothelial cells to grow along the length of the implant could prove beneficial. However, until we are able to document robust axon growth

simultaneous with the establishment of vasculature, we can not confirm this suspicion.

Chapter 5

Future Modifications of Electrospun Spinal Cord Implants

Spinal cord injuries directly impact over 250,000 individuals nationwide, diminishing quality of life considerably. Those who suffer from spinal cord injuries suffer from a myriad of problems, including but not limited to paralysis, loss of sensation, loss of bladder and bowel control, and loss of control over the sex organs. The pathology of spinal cord injuries creates a complex problem that to date has had little success in treating. Trauma to the spinal cord in both human and animal models results in necrosis in and around the site of injury. Over weeks to months, a fluid filled cyst often forms as an endpoint to the process. This cyst represents a physical impediment to axon and functional recovery. Inhibitory molecules are present throughout the cord following injury. Neurons who have undergone cell death are unable to upkeep their myelinated axons, which begin to degrade. This myelin debris is inhibitory to regenerating axons. In addition, inhibitory compounds are also released by reactive astrocytes in the area. A combinatorial strategy addressing multiple obstacles at once appears to offer potential for a meaningful functional outcome. Our lab utilized a novel approach in electrospinning a 3-d matrix and adding trophic as well as enzymatic support. Our electrospun matrices were able to be spun in proportion to the rat spinal cord, with its fibers aligned longitudinally and capable of directing axon growth. Additionally, we were able to supplement these electrospun matrices with

alginate beads containing viable neurotrophic growth factors and other compounds eliciting neuroprotective or neuroregenerative effects.

The electrospun matrices demonstrated were tested with a battery of *in vitro* tests until finally placed into animals. Implants were placed into rats who received complete transections of their spinal cords at the T8-T10 level. Rats given implants showed an increase in the quality of their hind limb movements. This exciting revelation led to an attempt to correlate the increased movements to the histology. The primary focuses were to elucidate the monofilament integration into the ECM and host tissue, the presence of axons in the matrix, the axon tract preservation above and below the level of the injury, and how our implant affected vascular supply. What we discovered was that our PDS monofilaments interacted seamlessly with the host tissues and instigated a cellularity complete through the injury site. This proved to be a crucial success for one of the primary purposes of the implant, to create a substrate that could fill a cavity in a spinal cord injury. Indeed, axons could be found throughout the extent of the implant. Loss of spinal cord architecture was observed, as well as a considerably decreased number of axons when compared to an uninjured spinal cord. Above and below the level of the lesion, axon tracts appear to have degraded at differential rates. This is significant due to the fact that little is known about the hardiness of specific axon tracts following injury. Generally, it appears that myelinated axons attached to the somas undergo far less myelin degradation, whereas detached myelinated axons are greatly degraded. Some axon tracts appear to show little regenerative capacity regardless of distance from soma. All in all, more experiments need to be done

assessing individual axon tracts in relation to their distance from the spinal cord transection. Beyond axons, we also discovered that cellular infiltration readily penetrated into the pores between the electrospun fibers, and ECM was laid down right up to the fibers. Even more encouraging is the fact that certain cells appear to use these monofilaments for structural support. Endothelial cells were found to wrap these monofilaments throughout our implants. Further evidence demonstrated red blood cells found in cross section through the lumen of these endothelial cells, as well as lines of RBC's found in longitudinal sections of the implant. The restoration of vascular supply supports the cellularization and potential for axon growth.

This experiment demonstrated the vast potential of these electrospun matrices. Not only were these electrospun matrices viable bridges for axons to grow on, but they also appeared to aid ingrowth of endothelial cells in reestablishing a functional vascular supply. As expected, these bridges were anti-pyrogenic and anti-antigenic.

As a result of the previous experiment showing such promising results, we perceived a novel method to enhance these matrices. A problem with the first implant was the potential for cells foreign to the CNS to enter the bridge and disrupt axonal growth. We hypothesized that fibroblasts that could enter the graft from the dorsal or ventral aspect would repel and perturb the growth of axons through the area of infiltration. We electrospun a PGLA coat over the PDS matrix to prevent fibroblastic infiltration. These PGLA capsules were also notable for being anti-pyrogenic and were used successfully in the PNS. These novel implants were utilized in vivo, with the expectation that axons able to enter the implant would now have no roadblocks

preventing linear growth to the opposing side. Unfortunately, few axons were able to enter the implant. There were many ideas for this misstep. Clearly the only engineering factor that changed was the addition of the PGLA capsule. This PGLA capsule may elicit a different response in an injury to the CNS then an injury to the PNS. If the PGLA were responsible for the additional inflammation, it would explain the fibroblastic capsule surrounding the implant. This may not be the answer, as concurrent to the design of the new implant; the laboratory lost the neurosurgeon responsible for the surgeries performed in the past. Replacing this neurosurgeon was no simple task, and the loss of his expertise on performing spinal cord transections may have resulted in animals receiving excess trauma to the spinal cord and meninges. This excess trauma to the area may have increased inflammation to the area of implantation, which would have increased fibroblastic infiltration to the area. We believe fibroblasts are the main villain in this experiment. Ultimately, the laboratory will return to the model of implant that has shown previous success in the past, and eliminate the PGLA capsule. This will allow us to discern which variable is responsible for the increased fibroblastic infiltration. While axons were unable to enter the matrix, this did not stop the implant from showing abundant cellularity within 3 weeks of implantation. Compared to the 12 week survival time of the first generation of implant, at 3 weeks, far less ECM has been laid down. Large gaps were prevalent throughout these matrices, and monofilaments were difficult to identify. This is confusing as the monofilaments should be omnipresent within the matrix. Evidence could be seen demonstrating the original orientation of fibers within the matrix; however these fibers are lost through the rest of

the cross sections. This may show that the EM process itself may degrade our monofilaments, preventing us from successfully seeing them at the LM level. While monofilaments may be degraded in vivo or following tissue processing, there is no denying the vascular network that has been formed. 3 weeks post injury; there is an abundance of vascular support being generated. As seen in the previous figure, there are blood vessels of all different stages of development present. This is a fascinating method for creating functional vasculature.

While this experiment with second generation PGLA coated PDS capsules did not offer functional recovery or axons in the implant, the future remains bright. In subsequent experiments, we plan to remove this PGLA coat and return to the model that was successful. We are currently investigating methods to cellularize these electrospun fibers, so that we may fortify them with astrocytes or schwann cells. Additionally, we are also investigating methods to utilize growth factor gradients to direct axons across the bridge with lower and lower concentrations, so that these axons will have no stimulus within the bridge. Future experiments will analyze the axon tract degradation rates and survivability in the days to weeks following the transection. Hardier axon tracts may exhibit greater potential for regeneration, and if this is the case, then specific growth factors would be needed in gradient or non gradient form throughout the implant. If axons are able to course the implant and reach the other side, neurotrophic factors must be released from the peripheral targets to coax those axons off. Exercise rehabilitation is an excellent subsequent step, as exercise rehab has been shown to increase release of BDNF and other growth factors. Additionally, exercise rehab may

help in maintaining motor end plates, muscle tone, and weight control in future rats. Finally, as we continue to investigate spinal cord injuries and utilize the complete transection model of injury, our surgical process will become further and further refined to the point where we will have a surgeon that is able to minimally affect the spinal cord and tissues, creating a much less traumatic injury. It has been shown that sealing the dura mater following surgery improves functional outcome.

There is hope in the future that we will have the tools and experience necessary to perform a perfectly reproducible surgery that exhibits minimal trauma to the animal and preserves the dura. The implant will have neurotrophic support targeting different axon tracts in gradients that promote axon growth through the implants to the other end. Trophic factors and guidance molecules stemming from exercise rehabilitation induced neurotrophin release would facilitate axonal exit from the implant. The future looks promising in the field of spinal cord injury.

List of References

Akiyama Y, Radtke C, Kocsis JD. Remyelination of the rat spinal cord by transplantation of identified bone marrow stromal cells. J Neurosci. 2002 Aug 1;22(15):6623-30.

Apostolova, I., Irintchev, A., Schachner, M., 2006. Tenascin-R restricts posttraumatic remodeling of motorneuron innervation and functional recovery after spinal cord injury in adult mice. J. Neurosci. 26, 7849-7859

Arendt T, Bruckner MK, Krell T, Pagliusi S, Kruska L, Heumann R. 1995. Degeneration of rat cholinergic basal forebrain neurons and reactive changes in nerve growth factor expression after chronic neurotoxic injury. II. Reactive expression of the nerve growth factor gene in astrocytes. *Neuroscience* 65:647–59

Ayres CE, Jha BS, Sell SA, Bowlin GL, Simpson DG. Nanotechnology in the design of soft tissue scaffolds: innovations in structure and function. Wiley Interdiscip Rev Nanomed Nanobiotechnol. 2010 Jan;2(1):20-34. Review

Ayres CE, Jha BS, Meredith H, Bowman JR, Bowlin GL, Henderson SC, Simpson DG. Measuring fiber alignment in electrospun scaffolds: a user's guide to the 2D fast Fourier transform approach. J Biomater Sci Polym Ed. 2008;19(5):603-21. Review.

Beeh KM, Kornmann O, Buhl R, Culpitt SV, Giembycz MA, Barnes PJ. Neutrophil chemotactic activity of sputum from patients with COPD: role of interleukin 8 and leukotriene B4. Chest. 2003 Apr;123(4):1240-7.

Behzadian MA, Wang XL, Jiang B, Caldwell RB. Angiostatic role of astrocytes: suppression of vascular endothelial cell growth by TGF-beta and other inhibitory factor(s). Glia. 1995 Dec;15(4):480-90.

Blight AR. Delayed demyelination and macrophage invasion: a candidate for secondary cell damage in spinal cord injury. Cent Nerv Syst Trauma. 1985;2:299 –315.

Blight AR. Macrophages and inflammatory damage in spinal cord injury. J Neurotrauma. 1992;9(suppl 1):S83-S91.

Blight AR, Cohen TI, Saito K, Heyes MP. Quinolinic acid accumulation and functional deficits following experimental spinal cord injury. *Brain.* 1995;118(pt 3):735–752.

Boland ED, Coleman BD, Barnes CP, Simpson DG, Wnek GE, Bowlin GL. Electrospinning polydioxanone for biomedical applications. Acta Biomater. 2005 Jan;1(1):115-23.

Bothwell M. 1995. Functional interactions of neurotrophins and neurotrophin receptors. Annu. Rev. Neurosci. 18:223–53

Bowlin G.L., Pawlowski K.J., Stitzel J.D., Boland E.D., Simpson D.G., Fenn J.B. et al. (2002) Electrospinning of polymer scaffolds for tissue engineering. In Lewandrowski K., Wise D., Trantolo D., Gresser J., Yaszemski M. ad Altobelli D. (eds) Tissue engineering and biodegradable equivalents: scientific and clinical applications. Marcel Dekker, pp.165-178.

Bradbury E.J., Moon L.D., Popat R.J., King V.R., Bennett G.S., Patel P.N., Fawcett J.W., McMahon S.B. Chondroitinase ABC promotes functional recovery after spinal cord injury. Nature. 2002 Apr 11;416(6881):631-40

Brittis PA, Canning DR, Silver J. Chondroitin sulfate as a regulator of neuronal patterning in the retina. Science. 1992 Feb 7;255(5045):733-6.

Butte MJ, Hwang PK, Mobley WC, Fletterick RJ. 1998. Crystal structure of neurotrophin-3 homodimer shows distinct regions are used to bind its receptors. Biochemistry 37:16846–52

Cafferty W.B., Bradbury E.J., Lidierth M., Jones M., Duffy P.J., Pezet S., McMahon S.B. Chondroitinase ABC-mediated plasticity of spinal sensory function. Neurosci. 2008 Nov 12;28(46):11998-2009.

Chandel NS, Maltepe E, Goldwasser E, Mathieu CE, Simon MC, Schumacker PT. Mitochondrial reactive oxygen species trigger hypoxia-induced transcription. Proc Natl Acad Sci U S A. 1998 Sep 29;95(20):11715-20.

Chandel NS, McClintock DS, Feliciano CE, Wood TM, Melendez JA, Rodriguez AM, Schumacker PT. Reactive oxygen species generated at mitochondrial complex III stabilize hypoxia-inducible factor-1alpha during hypoxia: a mechanism of O2 sensing. J Biol Chem. 2000 Aug 18;275(33):25130-8.

Chow W.N., Simpson D.G., Bigbee J.W., Colello R.J. Evaluating neuronal and glial growth on electrospun polarized matrices: bridging the gap in percussive spinal cord injuries. Neuron Glia Biol. 2007 May;3(2):119-126.

Chollet-Martin S, Jourdain B, Gibert C, Elbim C, Chastre J, Gougerot-Pocidalo MA. Interactions between neutrophils and cytokines in blood and alveolar spaces during ARDS. Am J Respir Crit Care Med. 1996 Sep;154(3 Pt 1):594-601.

Cortes M, Baria AT, Schwartz NB. Sulfation of chondroitin sulfate proteoglycans is necessary for proper Indian hedgehog signaling in the developing growth plate. Development. 2009 May;136(10):1697-706. Epub 2009 Apr 15.

Diener PS, Bregman BS. Neurotrophic factors prevent the death of CNS neurons after spinal cord lesions in newborn rats. Neuroreport. 1994 Oct 3;5(15):1913-7.

Dobrowsky RT, Jenkins GM, Hannun YA. 1995. Neurotrophins induce sphingomyelin hydrolysis. Modulation by co-expression of p75NTR with Trk receptors. J. Biol. Chem. 270:22135–42

Dobrowsky RT, Werner MH, Castellino AM, Chao MV, Hannun YA. 1994. Activation of the sphingomyelin cycle through the low-affinity neurotrophin receptor. Science 265:1596–99

Dougherty KD, Dreyfus CF, Black IB. Brain-derived neurotrophic factor in astrocytes, oligodendrocytes, and microglia/macrophages after spinal cord injury. Neurobiol Dis. 2000 Dec;7(6 Pt B):574-85.

Dusart I, Schwab ME. Secondary cell death and the inflammatory reaction after dorsal hemisection of the rat spinal cord. Eur J Neurosci. 1994;6:712–724

Fitch, M.T., Silver, J., 2001. Astrocytes are dynamic participants in central nervous system development and injury responses. In: Jessen, K.R., Richardson, W.D. (Eds.), Glial Cell Development: Basic Principles and Clinical Relevance. Oxford University Press, London, pp. 263–269.

Fitch, M.T., Doller, C., Combs, C.K., Landreth, G.E., Silver, J., 1999. Cellular and molecular mechanisms of glial scarring and progressive cavitation: in vivo and in vitro analysis of inflammation-induced secondary injury after CNS trauma. J. Neurosci. 19, 8182–8198.

Fridrikh SV, Yu JH, Brenner MP, Rutledge GC. Controlling the fiber diameter during electrospinning. Phys Rev Lett. 2003 Apr 11;90(14):144502. Epub 2003 Apr 8.

Goto F, Goto K, Weindel K, and Folkman J. Synergistic effects of vascular endothelial growth factor and basic fibroblast growth factor on the proliferation and cord formation of bovine capillary endothelial cells within collagen gels. Lab Invest 69: 508–517, 1993

Hagino, S., Iseki, K., Mori, T., Zhang, Y., Hikake, T., Yokoya, S., Takeuchi, M., Hasminoto, H., Kikuchi, S., Wanaka, A., 2003. Slit and glypican-1 mRNAs are coexpressed in the reactive astroycytes of the injured adult brain. Glia 42, 130-138

Han S, Arnold SA, Sithu SD, Mahoney ET, Geralds JT, Tran P, Benton RL, Maddie MA, D'Souza SE, Whittemore SR, Hagg T. Rescuing vasculature with intravenous angiopoietin-1 and alpha v beta 3 integrin peptide is protective after spinal cord injury. Brain. 2010 Apr;133(Pt 4):1026-42.

Hickey MM, Simon MC. Regulation of angiogenesis by hypoxia and hypoxia-inducible factors. Curr Top Dev Biol. 2006;76:217-57.

Hirschberg DL, Yoles E, Belkin M, Schwartz M. Inflammation after axonal injury has conflicting consequences for recovery of function: rescue of spared axons is impaired but regeneration is supported. *J Neuroimmunol*. 1994;50:9 –16.

Houle JD, Tom VJ, Mayes D, Wagoner G, Phillips N, Silver J. Combining an autologous peripheral nervous system "bridge" and matrix modification by chondroitinase allows robust, functional regeneration beyond a hemisection lesion of the adult rat spinal cord. J Neurosci. 2006 Jul 12;26(28):7405-15.

Huang W.C., Kuo W.C., Hsu S.H., Cheng C.H., Liu J.C., Cheng H. Gait analysis of spinal cord injured rats after delivery of chondroitinase ABC and adult olfactory mucosa progenitor cell transplantation. Neurosci Lett. 2010 Mar 19;472(2):79-84. Epub 2010 Jan 15.

Ibanez CF, Ebendal T, BarbanyG, Murray-Rust J, Blundell TL, Persson H. 1992. Disruption of the low affinity receptor-binding site in NGF allows neuronal survival and differentiation by binding to the trk gene product. *Cell* 69:329–41

Krenz NR, Weaver LC. Nerve growth factor in glia and inflammatory cells of the injured rat spinal cord. J Neurochem. 2000 Feb;74(2):730-9.

Lee H., McKeon R.J., Bellamkonda R.V. Sustained delivery of thermostabilized chABC enhances axonal sprouting and functional recovery after spinal cord injury. Proc Natl Acad Sci U S A. 2010 Feb 23;107(8):3340-5. Epub 2009 Nov 2.

Lemons ML, Howland DR, Anderson DK. Chondroitin sulfate proteoglycan immunoreactivity increases following spinal cord injury and transplantation. Exp Neurol. 1999 Nov;160(1):51-65.

Levi-Montalcini R, Skaper SD, Toso RD, Petrelli L, Leon A. 1996. Nerve growth factor: from neurotrophin to neurokine. *Trends Neurosci.* 19:514–20

Levi-Montalcini R, Toso RD, Valle FD, Skaper SD, Leon A. 1995. Update of the NGF saga. *J. Neurol. Sci.* 130:119–27

Li Y, Field PM, Raisman G. Repair of adult rat corticospinal tract by transplants of olfactory ensheathing cells. Science. 1997 Sep 26;277(5334):2000-2.

Lu X, Richardson PM. Inflammation near the nerve cell body enhances axonal regeneration. *J Neurosci*. 1991;11:972–978.

Matsumoto T and Claesson-Welsh L. VEGF receptor signal transduction. *Sci STKE* 2001: RE21, 2001.

Mautes AE, Weinzierl MR, Donovan F, Noble LJ. Vascular events after spinal cord injury: contribution to secondary pathogenesis. Phys Ther. 2000 Jul;80(7):673-87.

McDonald JW, Liu XZ, Qu Y, Liu S, Mickey SK, Turetsky D, Gottlieb DI, Choi DW. Transplanted embryonic stem cells survive, differentiate and promote recovery in injured rat spinal cord. Nat Med. 1999 Dec;5(12):1410-2.

McKeon, R.J., Schreiber, R.C., Rudge, J.S., Silver, J., 1991. Reduction of neurite outgrowth in a model of glial scarring following CNS injury is correlated with the expression of inhibitory molecules on reactive astrocytes. J. Neurosci. 11, 3398- 3411.

Molea G., Schonauer F., Bifulco G., D'Angelo D. Comparative study on biocompatibility and absorption times of three absorbable monofilament suture materials (Polydioxanone, Poliglecaprone 25, Glycomer 631). Br J Plast Surg. 2000 Mar;53(2):137-41.

Morgenstern DA, Asher RA, Fawcett JW. Chondroitin sulphate proteoglycans in the CNS injury response. Prog Brain Res. 2002;137:313-32.

Myer, D.J., Gurkoff, G.G., Lee, S.M., Hovda, D.A., Sofroniew, M.V., 2006. Essential protective roles of reactive astrocytes in traumatic brain injury. Brain 129, 2761–2772.

Norenberg, M.D., Astroycyte responses to CNS injury. J. Neuropathol. Exp. Neurol. 1994;53, 213-220

Noushi F, Richardson RT, Hardman J, Clark G, O'Leary S. Delivery of neurotrophin-3 to the cochlea using alginate beads. Otol Neurotol. 2005 May;26(3):528-33.

Pasterkamp, R.J., Anderson, P.N., Vehaagen, J., 2001. Peripheral nerve injury fails to induce growth of lesioned ascending dorsal column axons into spinal cord scar tissue expressing the axon repellent Semaphorin3A. Eur. J. Neurosci. 13, 457-471.

Perry VH, Brown M. Macrophages and nerve regeneration. *Curr Opin Neurobiol*. 1992:2:679–682.

Pitts AF, Miller MW. 2000. Expression of nerve growth factor, brain-derived neurotrophic factor, and neurotrophin-3 in the somatosensory cortex of the mature rat: coexpression with high-affinity neurotrophin receptors. J. Comp. Neurol. 418:241–54

Popovich PG, Horner PJ, Mullin BB, Stokes BT. A quantitative spatial analysis of the blood-spinal cord barrier, I: permeability changes after experimental spinal contusion injury. *Exp Neurol*. 1996;142:258 –275.

Reese TS, Karnovsky MJ. Fine structural localization of a bloodbrain barrier to exogenous peroxdiase. *J Cell Biol.* 1967;34:207–217.

Reier P.J., Bregman B.S., Wujek, J.R. Intraspinal transplantation of embryonic spinal cord tissue in neonatal and adult rats. J. Comp. Neurol. 1986 May 15; 247(3):275-96

Rosenberg GA. Matrix metalloproteinases in brain injury. *J Neurotrauma.* 1995;12:833– 842

Rosenstein JM, Krum JM. New roles for VEGF in nervous tissue--beyond blood vessels. Exp Neurol. 2004 Jun;187(2):246-53.

Tisay K.T., Key B., The extracellular matrix modulates olfactory neurite outgrowth on ensheathing cells. J Neurosci. 1999 Nov 15;19(22)9890-9

Saltiel AR, Decker SJ. Cellular mechanisms of signal transduction for neurotrophins. Bioessays. 1994 Jun;16(6):405-11.

Schnell L, Fearn S, Klassen H, Schwab ME, Perry VH. Acute inflammatory responses to mechanical lesions in the CNS: differences between brain and spinal cord. Eur J Neurosci 1999a; 11: 3648–3658.

Stiefel MF, Tomita Y, Marmarou A. Secondary ischemia impairing the restoration of ion homeostasis following traumatic brain injury. J Neurosurg. 2005 Oct;103(4):707-14.

Stitzel JD, Pawlowski KJ, Wnek GE, Simpson DG, Bowlin GL. Arterial smooth muscle cell proliferation on a novel biomimicking, biodegradable vascular graft scaffold. J Biomater Appl. 2001 Jul;16(1):22-33.

Sun T, Mai S, Norton D, Haycock JW, Ryan AJ, MacNeil S. Self-organization of skin cells in three-dimensional electrospun polystyrene scaffolds. Tissue Eng. 2005 Jul-Aug;11(7-8):1023-33.

Tang X, Davies JE, Davies SJ. Changes in distribution, cell associations, and protein expression levels of NG2, neurocan, phosphacan, brevican, versican V2, and tenascin-C during acute to chronic maturation of spinal cord scar tissue. J Neurosci Res. 2003 Feb 1;71(3):427-44.

Telemeco T.A., Ayres C., Bowlin G.L., Wnek G.E., Boland E.D., Cohen N., Baumgarten C.M., (...), Simpson D.G. Regulation of cellular infiltration into tissue engineering scaffolds composed of submicron diameter fibrils produced by electrospinning (2005) Acta Biomaterialia, 1(4), pp. 377-385.

Tidball J.G., Inflammatory cell response to acute muscle injury. Med Sci Sports Exerc. 1995 Jul;27(7):1022-32.

Tsai EC, Dalton PD, Shoichet MS, Tator CH. Synthetic hydrogel guidance channels facilitate regeneration of adult rat brainstem motor axons after complete spinal cord transection. J Neurotrauma. 2004 Jun;21(6):789-804.

Vejsada R, Sagot Y, Kato AC. Quantitative comparison of the transient rescue effects of neurotrophic factors on axotomized motoneurons in vivo. Eur J Neurosci. 1995 Jan 1;7(1):108-15.

von Wild KR, Brunelli GA. Restoration of locomotion in paraplegics with aid of autologous bypass grafts for direct neurotisation of muscles by upper motor neurons--the future: surgery of the spinal cord? Acta Neurochir Suppl. 2003;87:107-12.

Wamil AW, Wamil BD, Hellerqvist CG. CM101-mediated recovery of walking ability in adult mice paralyzed by spinal cord injury. *Proc Natl Acad Sci USA*. 1998;95:13188–13193.

Webber CA, Hyakutake MT, McFarlane S. Fibroblast growth factors redirect retinal axons in vitro and in vivo. Dev Biol. 2003 Nov 1;263(1):24-34.

Wen X, Tresco PA.Biomaterials. Fabrication and characterization of permeable degradable poly(DL-lactide-co-glycolide) (PLGA) hollow fiber phase inversion membranes for use as nerve tract guidance channels. 2006 Jul;27(20):3800-9. Epub 2006 Mar 27.

Whetstone WD, Hsu JY, Eisenberg M, Werb Z, Noble-Haeusslein LJ. Blood-spinal cord barrier after spinal cord injury: relation to revascularization and wound healing. J Neurosci Res. 2003 Oct 15;74(2):227-39.

Wilby MJ, Muir EM, Fok-Seang J, Gour BJ, Blaschuk OW, Fawcett JW. N-Cadherin inhibits Schwann cell migration on astrocytes. Mol Cell Neurosci. 1999 Jul;14(1):66-84.

Xu XM, Guénard V, Kleitman N, Bunge MB. Axonal regeneration into Schwann cell-seeded guidance channels grafted into transected adult rat spinal cord. J Comp Neurol. 1995 Jan 2;351(1):145-60.

Zhang Z, Guth L. Experimental spinal cord injury: Wallerian degeneration in the dorsal column is followed by revascularization, glial proliferation, and nerve regeneration. *Exp Neurol*. 1997;147: 159–171.

Zhang B, Dietrich UM, Geng JG, Bicknell R, Esko JD, Wang L. Repulsive axon guidance molecule Slit3 is a novel angiogenic factor. Blood. 2009 Nov 5;114(19):4300-9. Epub 2009 Sep 9.

Zhang HT, Gao ZY, Chen YZ, Wang TH. Temporal changes in the level of neurotrophins in the spinal cord and associated precentral gyrus following spinal hemisection in adult Rhesus monkeys. J Chem Neuroanat. 2008 Dec;36(3-4):138-43. Epub 2008 Jul 22.

Vita

Charles Shin Lin was born in Los Alamitos, California on August 4, 1985. He attended the University of California, Davis from 2003-2007 and received a Bachelors degree in Science in 2007. He began his work towards a Master of Science Fall of 2008 at Virginia Commonwealth Science Fall of 2008 at Virginia Commonwealth University.